ANNUAL REVIEWS

Annual Review of Fluid Mechanics

Advances in Bioconvection

Martin A. Bees

Department of Mathematics, University of York, York YO19 5DD, United Kingdom; email: martin.bees@york.ac.uk

Annu. Rev. Fluid Mech. 2020. 52:449–76

The *Annual Review of Fluid Mechanics* is online at fluid.annualreviews.org

https://doi.org/10.1146/annurev-fluid-010518-040558

Keywords

hydrodynamic instability, patterns, biased swimming microorganisms, suspensions, gravitaxis, gyrotaxis, phototaxis, chemotaxis

Abstract

The term "bioconvection" describes hydrodynamic instabilities and patterns in suspensions of biased swimming microorganisms. Hydrodynamic instabilities arise from coupling between cell swimming behaviors; physical properties of the cells, such as density; and fluid flows. For instance, a combination of viscous and gravitational torques can lead to cells swimming toward downwelling fluid. If the cells are more dense than the fluid, then a gyrotactic instability results. Phototaxis describes the directed response of cells to light, which can also lead to instability. Bioconvection represents a classic system where macroscopic phenomena arise from microscopic cellular behavior in relatively dilute systems. There are ecological consequences for bioconvection and the mechanisms involved as well as potential for industrial exploitation. The focus of this review is on progress measuring and modeling gyrotactic and phototactic bioconvection. It builds on two earlier reviews of bioconvection and recent interest in active matter, describing progress and highlighting open problems.

1. INTRODUCTION

1.1. Collective Behavior

Taxis: directed movement of an organism in response to a stimulus

Kinesis: nondirectional movement of an organism in response to a stimulus

Gravitaxis: directed motility in response to gravity

Gyrotaxis: directed motility due to gravitational and viscous torques; typically, bottom-heavy cells swim toward downwelling regions

Phototaxis: directed motility in response to light

Rheotaxis: directed motility in response to the direction of fluid flow

Magnetotaxis: directed motility in response to a magnetic field

Chemotaxis: directed motility in response to a chemical gradient

Oxytaxis: chemotaxis with oxygen

Bioconvection (coined by Platt 1961) is a self-organized structure and flow that arises naturally when biased swimming microorganisms are left unstirred in liquid culture and is usually identified by patterns in cell concentration. In an investigation of patterns in *Euglena viridis*, Wager (1911) described earlier observations of other organisms by Nägeli (1860) and Sachs (1876). Typically, cell concentration patterns and fluid flow develop tens of seconds to minutes after mixing. Characteristic length scales are roughly two or three orders of magnitude larger than the size of individual organisms. The mechanisms are hydrodynamic instabilities mainly due to either the accumulation of non-neutrally buoyant cells that form unstable density gradients or an unstable swimming orientation field coupled to fluid flow gradients and cell concentration. **Figure 1** presents typical patterns obtained in the laboratory under controlled conditions for a range of species (Section 2).

Bioconvection has been described as an example of collective vortex behavior, with parallels for larger organisms (social insects, fish, and bats), and of stigmergy, describing mechanisms of coordination through the environment without direct interaction or communication (Delcourt et al. 2016). Complex structures emerge in the absence of planning or control. A natural question to ask then is, What is the function of bioconvection? Does it just appear in artificial environments, such as a laboratory? **Figure 1** presents bioconvection patterns discovered in natural settings. It is much easier for individuals to meet (to exchange DNA; Demetsmets et al. 1990) in two-dimensional (2D) surfaces or 1D plumes, and macroscale fluid flow mixes nutrients (Bees & Croze 2014). Bees & Croze (2010) have argued that in deep suspensions where phototrophic cells become light limited, the formation of long vertical plume structures may be advantageous for light transmission.

1.2. Individual Behavior

Key to the hydrodynamic instability mechanism for bioconvection is individual behavior driving cell accumulation and fluid flow. Many cells exhibit either passive or active motile responses to their environment (a taxis or kinesis). For example, many algae (e.g., *Chlamydomonas* spp., *Dunaliella* spp.) and protozoa (e.g., *Paramecium* spp.) are gravitactic, swimming upward on average in the absence of other stimuli. In the presence of an upper surface, cells accumulate, balancing mean upward swimming with a diffusive flux. As the cells are typically more dense than the surrounding fluid, an overturning instability can arise (**Figure 2*c***). A balance between gravitational and viscous torques (**Figure 2*a***) is termed gyrotaxis, which is often observed when cells are bottom heavy or subject to a sedimentation torque, leading cells to swim toward downwelling and away from upwelling regions (**Figure 2*b***) (Section 4). Cell accumulation drives the fluid to sink more quickly, resulting in focused plume structures that are evident in nonmixed culture flasks or downwelling Poiseuille flow (Kessler 1985b, Bees & Croze 2010). A gyrotactic instability does not require an upper surface or vertical density gradient. Phototaxis describes an affinity for cells to swim toward (positive) or away from (negative) a light source, which can also drive instabilities. [This is distinct from a photophobic response to a step change in light intensity, which causes a brief cessation of motion followed by a period of altered motility (Diehn et al. 1977).] Other taxes include rheotaxis, magnetotaxis, and chemotaxis, particularly oxytaxis (sometimes referred to as aerotaxis).

Swimming microorganisms propel themselves with a variety of mechanisms (Lauga & Powers 2009). Methods range from swimming with a single thin whiplike structure, called a flagellum, to coordinating the movement of many appendages, such as for the ciliated protozoan *Paramecium*, or changing body shape. The key to swimming at small Reynolds number is to ensure nonreciprocal body kinematics [which means that the swimming stroke should not be invariant under time

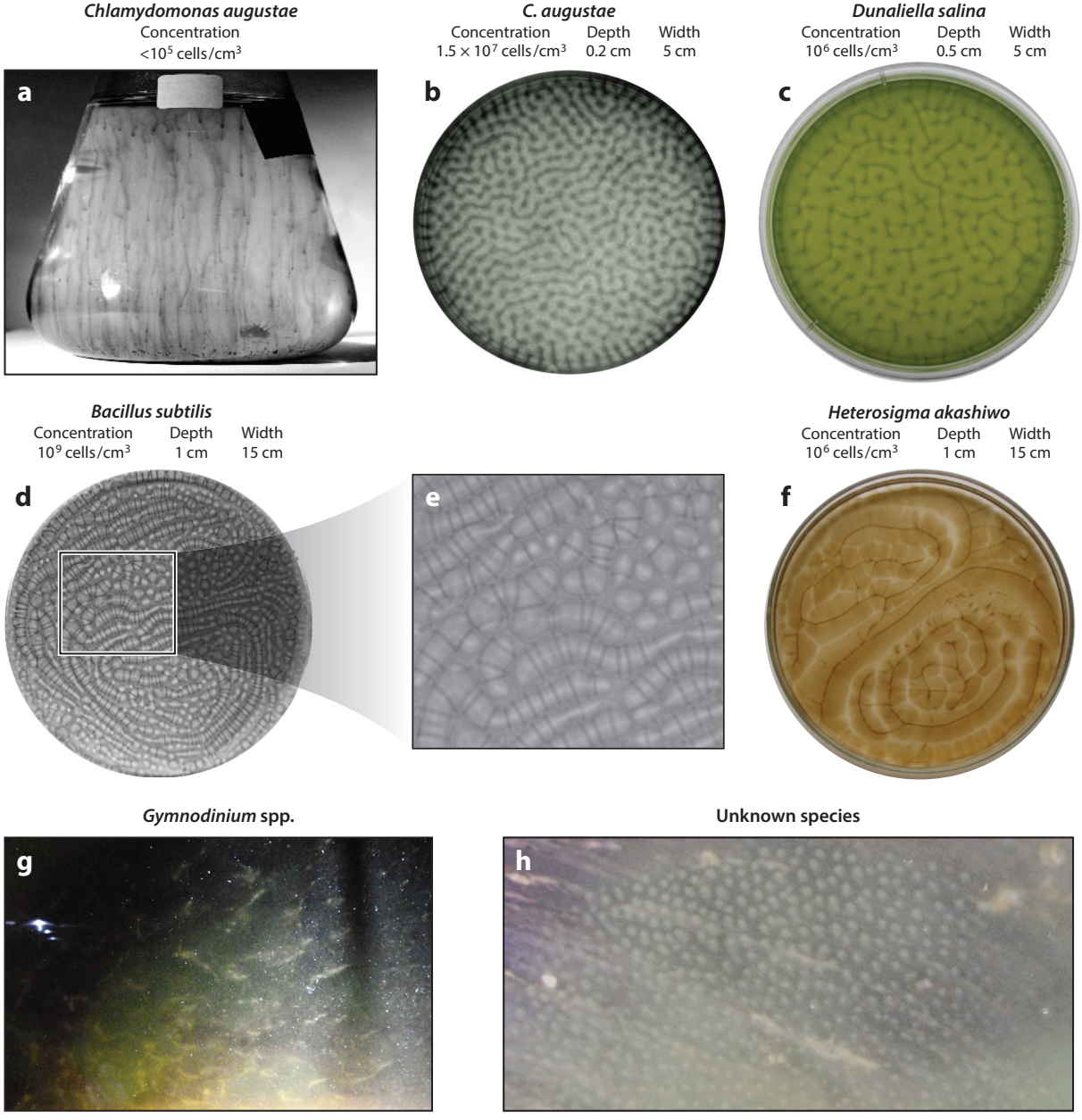

Figure 1

Bioconvection patterns, where dark regions indicate high cell concentration, except for panels *d*, *e*, *g*, and *h*, where it is the opposite. (*a*) Plumes in a suspension of the freshwater green alga *Chlamydomonas augustae* (née *C. nivalis*) in a culture flask. (*b–f*) Patterns from above: (*b*) *C. augustae*; (*c*) the halophile green alga and biofuel candidate *Dunaliella salina*; (*d*) labyrinthine patterns due to the oxytactic bacterium *Bacillus subtilis*, magnified in panel *e*, illustrating small-scale structures such as dark bands formed along the rolls; and (*f*) the marine alga and harmful algal bloom species *Heterosigma akashiwo*. (*g*) Bioconvection in a plant pot in a natural bloom of the dinoflagellate *Gymnodinium* (plumes are approximately 1 cm apart). (*h*) Bioconvection in a high intertidal pool (species unknown), estimated as 1–2 mm between plumes. Panels adapted or reprinted with permission from (*a*) Williams & Bees (2011b); (*b*) Bees (1996); (*c*) Bees & Croze (2014); (*f*) Bearon & Grunbaum (2006), copyright 2006 AIP Publishing; and (*h*) Bearon & Grunbaum (2006), copyright 2006 AIP Publishing. Photo in panel *g* courtesy of O.A. Croze, University of Cambridge, and photo in panel *h* courtesy of K. Sebens, Friday Harbor Laboratories, University of Washington.

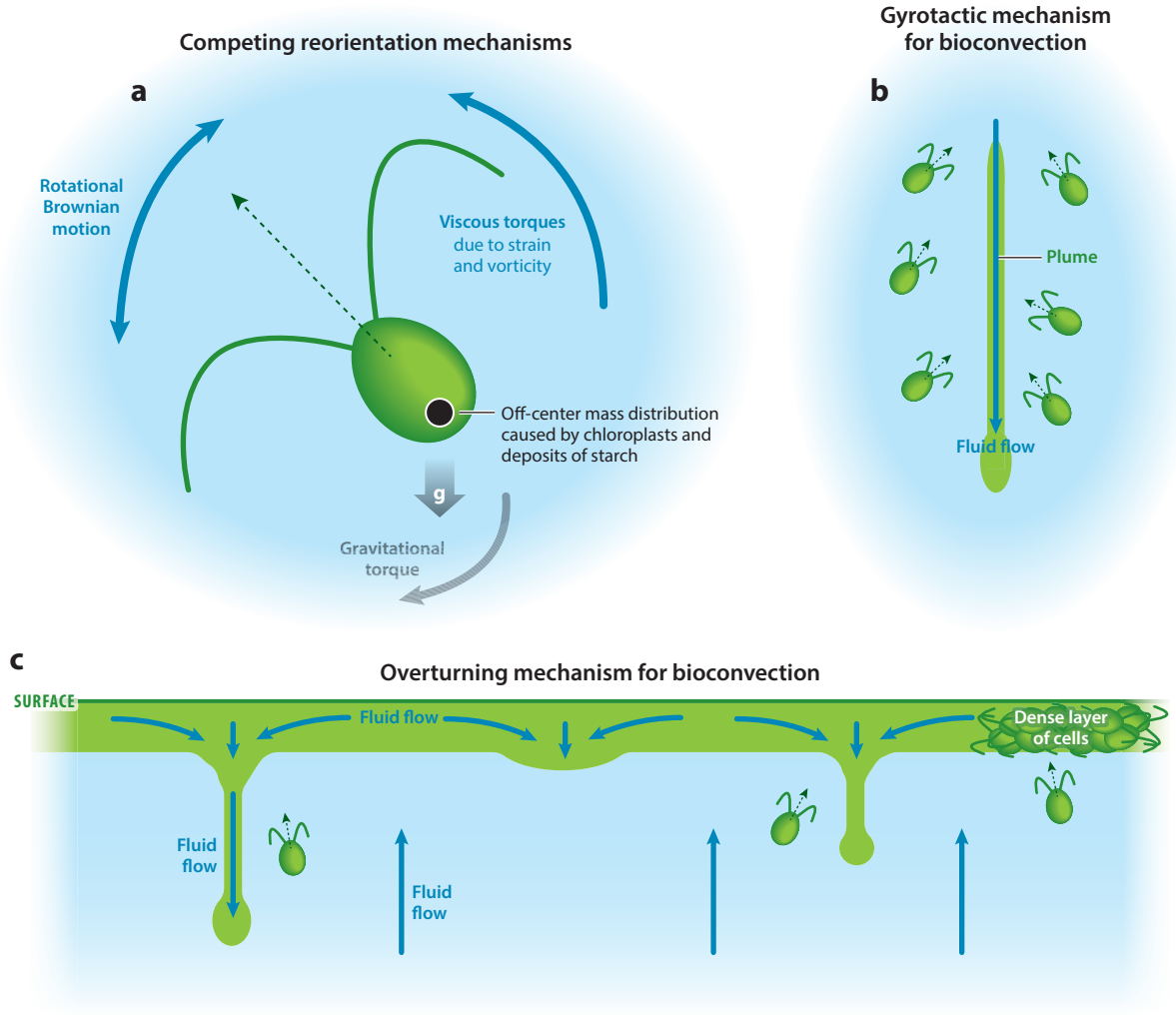

Figure 2

Mechanisms for gravitactic and gyrotactic bioconvection. (*a*) Viscous torques can act in opposition to a gravitational torque (or sedimentary torque) in the presence of rotational Brownian motion, tipping the cell to swim at an angle to gravity on average. (*b*) Bioconvection can arise from a gyrotactic mechanism, whereby tipped cells typically swim toward and accumulate in downwelling regions, driving further flow if the cells are not neutrally buoyant. (*c*) In an overturning mechanism, cells upswimming (downswimming) due to, for example, gravitaxis, chemotaxis, or phototaxis accumulate at an upper (lower) surface, which can create an unstable density profile if cells are negatively (positively) buoyant.

reversal, allowing for a nonlinear scaling of time and preserving the order of body configurations; see Lauga & Powers (2009)]. Such swimmers can be classified as pushers (as they push themselves forward by generating thrust at the rear; producing outward flow forward, backward, and in at the sides) or pullers (as they pull their body forward using their flagella; with flow opposite to that of a pusher). Pushers include spermatozoa; monotrichous bacteria such as *Escherichia coli*, with a single posterior flagellum beating with a planar or helical wave; and the peritrichously flagellated bacterium *Bacillus subtilis*. The classic example of a puller is the biflagellate alga *Chlamydomonas*, which swims with two anterior flagella with a breaststroke (or more accurately, the propagation of

bending waves along the flagella) at 50 Hz. Force-free swimming cells exhibit a stresslet flow with $|\mathbf{u}| \sim 1/r^2$ in the far field in three dimensions, whereas the gravitational force exerted on cells of different density to the fluid induces a Stokeslet flow in the far field with $|\mathbf{u}| \sim 1/r$ (Drescher et al. 2010). Near-field flows are, in general, more complex (e.g., **Figure 3*f***).

1.3. Relation to Other Areas

Isolated, freely swimming, and seemingly independent microorganisms switch their behavior to exhibit a wealth of interaction and communal structure when cells are in close proximity. This is epitomized by quorum-sensing communication within surface-associated bacterial colonies (Daniels et al. 2004) established from free-swimming cells and by communal growth and enhanced antibacterial resilience in biofilms (Flemming et al. 2016). Such communities consist of single or multiple species (Elias & Banin 2012) and are typically associated with exuded extracellular structure. A natural question is whether there is a more subtle increase of interaction and cooperation with cell concentration that emerges in dilute suspensions through the biased swimming behavior of microorganisms coupled to their common environment (e.g., Tuval et al. 2005). The field of active matter explores the concentrated end of the cell density spectrum where bacterial turbulent flows are found (Dunkel et al. 2013), and there is a clear correspondence with liquid crystals (Ramaswamy 2010). This review does not focus on these aspects.

The term "bioconvection" has traditionally been used to describe patterns and flows with cell concentrations at the dilute end of the spectrum (Platt 1961)—dilute in the sense that cells are many body lengths apart and the volume fraction is low (e.g., *Chlamydomonas* spp., with diameters less than 10 μm, form bioconvection patterns in petri dishes with concentrations of 10^6 cells/cm^3, yielding a volume fraction of 0.05% and a mean cell separation of 10 body diameters). Coupling between individuals is through macroscale hydrodynamic effects: Concurrently, cell accumulation and buoyancy drive flow, and flow advects concentration profiles and impacts swimming orientation. Microorganism-induced bulk stresses (due to swimming stroke) have long been included in this description (Pedley & Kessler 1990), and recent work has sought to explore semidilute regions of parameter space (Pedley 2010). "Bioconvection" describes instabilities and spatial structures without the close association required in active matter studies.

1.4. Potential Impact

There is considerable potential impact in industry for better understanding the behavior of suspensions of swimming microorganisms and the structures they generate (Bees & Croze 2014). Applications include extensive and intensive schemes for the production of biodiesel (lipids from stressed algae), synthesis of other products in photobioreactors, such as beta carotene, and gray water treatment. In these systems a significant issue is minimizing energy input [a third of costs is cell dewatering, potentially facilitated by cell focusing; e.g., see Kessler (1985b) and Bees & Croze (2014)]. Interestingly, behavior is a function of stress, which features strongly in algal H_2 production (Williams & Bees 2014). We need to move away from treating bacterial and algal bioreactors as chemical systems and embrace and utilize the biologically motivated biased swimming behavior of the microorganisms.

According to Smayda (1997), 90% of harmful algal bloom (HAB) species are flagellates, suggesting that swimming may confer some advantage, including pattern swimming (another name for bioconvection). Maximal cell concentrations in the HABs range over several orders of magnitude, exceeding 10^6 cells/cm^3 for brown tide species (Smayda 1997), although deleterious effects are evident for cell concentrations orders of magnitude less than this. It is plausible that localized

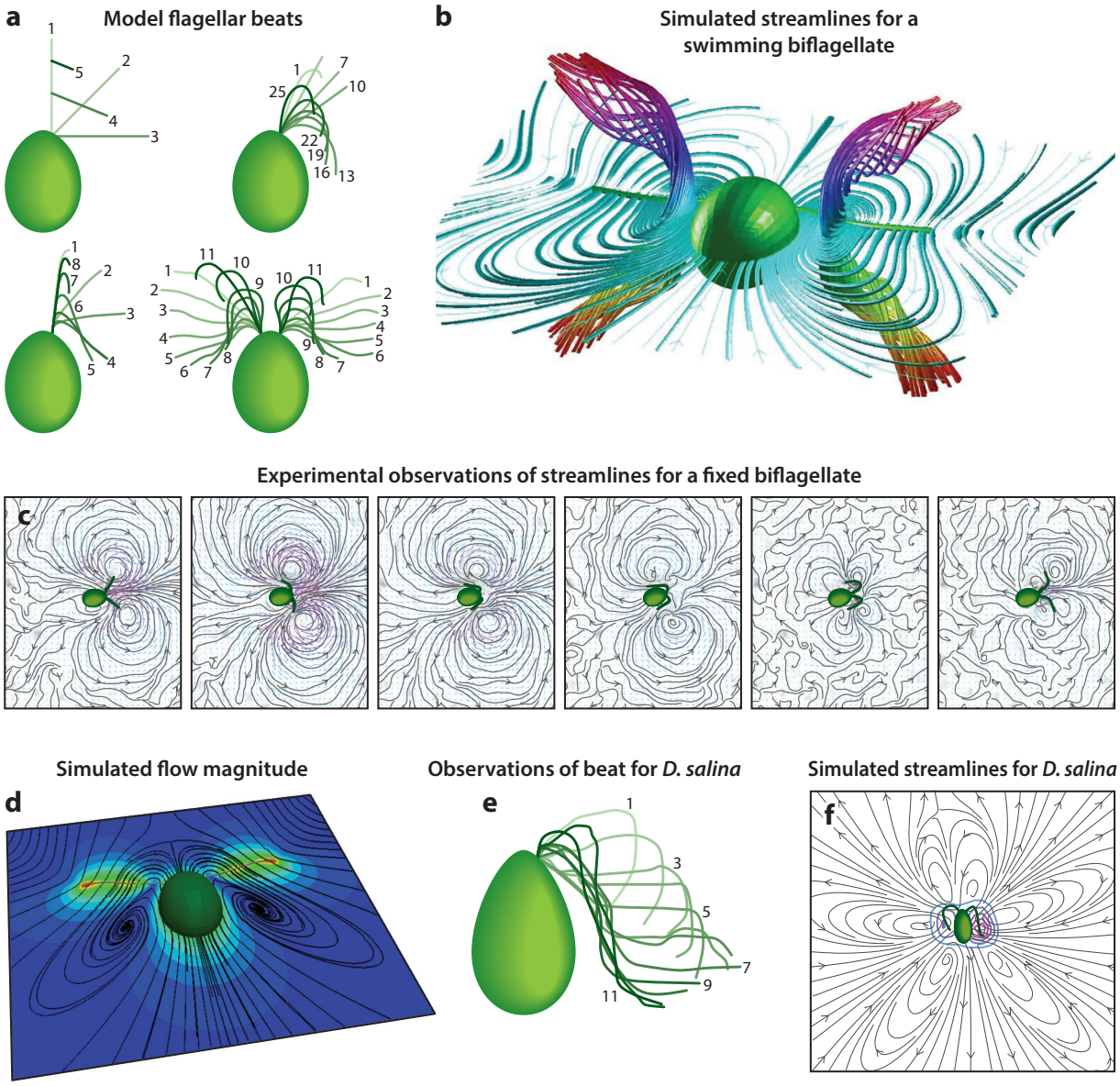

Figure 3

(*a*) Various flagella beats for *Chlamydomonas*. (*b*) Flow fields for a numerical biflagellate swimmer approaching the end of the effective stroke. The streamlines illustrate vortex formation, expelling fluid away from the flagellar plane. (*c*) Instantaneous fluid streamlines using particle image velocimetry for experimental observations of a single fixed cell of *Chlamydomonas reinhardtii* in a thin layer. Faint purple and blue arrows indicate the direction of the flow, with darker shades signifying greater magnitudes (also see Guasto et al. 2010). (*d*) Flow magnitude is high around the flagella and body. (*e*) The flagellar beat of *Dunaliella salina* is asynchronous; only one flagellum is plotted. (*f*) Simulations of *D. salina* reveal a complex near field. Panels adapted with permission from (*a*,*b*) O'Malley & Bees (2012) and (*c*,*e*,*f*) O'Malley (2011).

concentrations in blooms approach those of bioconvection experiments. Furthermore, built into the individual behavior are mechanisms for self-concentration (particularly gyrotaxis, phototaxis, and chemotaxis), which can lead to thin phytoplankton layers in shear flows or patchiness (e.g., Durham et al. 2013).

1.5. Scope of This Review

This article builds on two previous bioconvection reviews (Pedley & Kessler 1992, Hill & Pedley 2005) that document the close connection between experimental and theoretical results, noting also a recent review on theoretical aspects of active suspensions (Desai & Ardekani 2017). Pedley & Kessler (1992) laid the foundation for the subject area of bioconvection, which was updated by Hill & Pedley (2005) with developments from 1992 to 2005, particularly nonlinear theory, dispersion in shear, numerical solutions, and advances in modeling phototaxis, oxytaxis, and gyrotaxis. We do not attempt to replicate the discussion or comprehensive literature described in either review. Instead, beyond introductory material, the aim is to focus on literature since 2005, starting with experimental studies of bioconvection and their context (Section 2), setting the foundation for modeling approaches (Section 3), and moving on to modeling challenges, particularly gyrotactic bioconvection (Section 4) and phototactic bioconvection (Section 5), with a little discussion of oxytactic bioconvection (Section 6) and peripheral topics (Section 7). We conclude by discussing future issues.

2. EXPERIMENTAL MOTIVATION

2.1. Laboratory Observations

It is essential in a field such as bioconvection that experimental observations drive the development of theory and that any theoretical insights gained can be tested experimentally to challenge mechanistic understanding. There are now many observations of bioconvection [see Pedley & Kessler (1990) and Hill & Pedley (2005) for a more detailed discussion of early results].

Some of the first studies were by Wager (1911) with eukaryotic algae *E. viridis* and *Chlamydomonas* spp., the dinoflagellate *Glenodinium cinctum*, and bacteria of the genus *Spirillum*. Loeffer & Mefferd (1952) documented irregular aggregations that appear within a few seconds of shaking liquid cultures of *Euglena gracilis* or the ciliated protozoa *Tetrahymena pyriformis*.

Later observations with algae have employed *Chlamydomonas reinhardtii* and *Chlamydomonas augustae* (**Figure 1*a*,*b***; *C. augustae* is likely mistakenly classified in some studies as *Chlamydomonas nivalis*) (Kessler 1984, 1985a,b; Pedley et al. 1988; Pedley & Kessler 1990; Yamamoto et al. 1992; Bees & Hill 1997; Croze et al. 2010; Williams & Bees 2011b; Sato et al. 2018), *Dunaliella tertiolecta* (Pedley & Kessler 1992), and the biofuel candidate *Dunaliella salina* (**Figure 1*c***) (Bees & Croze 2014). Bioconvection patterns have been explored further with ciliated protozoa *Paramecium tetraurelia* (Kitsunezaki et al. 2007) and *Tetrahymena* spp. (Wille & Ehret 1968, Winet & Jahn 1972, Plesset & Winet 1974, Levandowsky et al. 1975, Childress et al. 1975, Pedley & Kessler 1992, Mogami et al. 2004); industrially relevant dinoflagellates, such as *Crypthecodinium cohnii* (Childress et al. 1975); toxic red tide dinoflagellates *Karenia mikimotoi* (Gentien et al. 2007) and *Alexandrium fundyense* (Persson & Smith 2013); and mixotrophic HAB species *Heterosigma akashiwo* (Bearon & Grunbaum 2006), which can decimate marine fish populations (Anderson et al. 2012).

The first quantitative analysis of bioconvection patterns was by Bees & Hill (1997). They used Fourier analysis to study the dependence of pattern wavelength on fluid depth and cell concentration in suspensions of the gyrotactic biflagellate *C. augustae* [also employed by others

(Czirok et al. 2000)]. Williams & Bees (2011b) extended the Bees & Hill (1997) approach to study a combination of gravitaxis, gyrotaxis, and phototaxis (Section 5). Wavelets have been employed to identify secondary modes (Almahmud 2016). In the case of *T. pyriformis*, Mogami et al. (2004) investigated the effect of increased gravity with a long-arm centrifuge. Results indicated that patterns are more readily formed, and existing patterns reduce their wavelength. Reduced-gravity experiments, using parabolic flight, were consistent with the opposite effect, although experimental time was limited to a couple of minutes (Mogami et al. 2001, Kage et al. 2011). In a hyperdense medium, Hosoya et al. (2010) found that *C. reinhardtii* accumulated at the bottom of the chamber, leading to an instability and upward-moving plumes (discussed also by Bees 1996), suggesting a reorientation mechanism that was dependent, to some degree, on viscous torques due to translation of an asymmetric body (see discussion in Section 4.1). A similar phenomenon was observed in a hyperdense medium illuminated from below (Sato et al. 2018).

For the alga *H. akashiwo*, Bearon & Grunbaum (2006) explored bioconvection patterns in a system with salinity stratification (see **Figure 1*f***). They found that in a weakly stratified fluid plume, structures of 20 cm could be obtained, and the addition of a low-salinity surface layer promoted dense surface aggregation, which could be used industrially to concentrate cells. Good agreement was obtained with linear stability analysis, with large salinity gradients suppressing the vertical extent of the perturbations. Karimi & Ardekani (2013) investigated this further with large-scale 3D numerical simulations of gyrotactic cells in the presence of thermal or solutal gradients and identified thresholds for the inhibition of bioconvection. Of particular importance was the Lewis number, Le, the ratio of thermal to cell diffusivity. With $\mathrm{Le} < 1$ in the case of solutally insulated boundaries, a buoyancy ratio (describing the relative importance of salinity and cell buoyancy forces) determined whether the stabilizing salinity gradient was sufficient to suppress bioconvection. However, for $\mathrm{Le} > 1$ bioconvection was robustly maintained with thermally insulated boundaries, but stratification thresholds were found with constant-temperature boundary conditions.

With the dinoflagellate *A. fundyense*, cell density–dependent patterns were observed only when the cells were in stationary phase but not in exponential growth phase, suggesting variations in taxes (Persson & Smith 2013). With microscopic observations it was found that cells in the plumes swam at twice the speed, increased contact rates, and changed direction three times more frequently compared to outside the plumes, suggesting a biological purpose for the structures. Gentien et al. (2007) investigated the common red tide dinoflagellate *K. mikimotoi*. This species produces a short-lived toxin that may help provide a competitive advantage but can also limit its own growth (autotoxicity). Cells typically accumulate at the top of a distilled water layer due to phototaxis. The authors found that there is a trade-off between cell accumulation at the upper boundary and autotoxicity; bioconvection promoted toxin dispersal away from the community of *K. mikimotoi*, reducing death rates and maintaining their competitive advantage.

Abe et al. (2017) found that they could control bioconvection flows in suspensions of *Salmonella* by releasing a chemoattractant at the tip of a capillary. In general, cell concentration in the vicinity of the capillary tip increased to a saturation level. The speed of the flow was mainly governed by the size of the accumulation region.

Tuval et al. (2005) described bioconvection in a sessile drop of *B. subtilis* (see also Janosi et al. 1998, Metcalfe & Pedley 1998, Mendelson 1999). Experiments and numerical results indicated that at first the bacteria migrated chemotactically up the oxygen gradient (oxytaxis) in the region near the curved fluid–air interface, generating an oxygen depletion layer of uniform thickness $l \approx 1$ mm and a cell accumulation layer of thickness $d \approx 100$ μm. The accumulation layer was observed to slide along the meniscus to the contact line, during which the layer became unstable to overturning instabilities and plume formation, with a length scale comparable to fluid depth. A chemotactic Boycott effect was said to occur due to the sloping surface in the region around the contact

line. (The classical Boycott effect enhances the settling of particles by the large-scale circulation that results from particle depletion at a tilted upper boundary.) This generates a large and persistent vortex that concentrates and traps cells near the contact line for many tens of minutes. The circulation is found to be strong enough that the uptake of oxygen into the suspension is significantly enhanced and even dominated by advection (i.e., a large Péclet number). The implication in this geometry is that bioconvection can alter the environmental conditions and promote colony growth, presenting a conclusion different from that of earlier studies in suspensions of constant depth (Janosi et al. 2002). Tuval et al. (2005) indicated that cell concentrations get very high in the contact region and that singular solutions at the contact line are possible in their model. Thus, they proposed that this geometrically mediated concentrative mechanism facilitates the formation of an immobilized region of cells that could initiate the formation and propagation of a biofilm.

Bioconvection is not limited to bacteria, protozoa, or algae. It has been observed in zoospores of the fungus-like plant pathogen *Phytophthora citricola* (Ochiai et al. 2011) with a gyrotactic mechanism. When unicellular motile propagules (zoospores) are released into the surrounding fluid, they self-organize into macroscale structures, driving fluid flow (termed pattern swimming). Ochiai et al. (2011) indicated that chemotaxis may be involved, and there are implications for cohort recruitment during infection.

2.2. In the Wild

Bioconvection is not confined to the laboratory. **Figure 1*g*,*h*** presents two serendipitously obtained photographs of bioconvection patterns. The first was found in a deep plant pot involving the dinoflagellate *Gymnodinium*, and the second, with an unknown species, was found in a high intertidal pool.

Sommer et al. (2017) provided compelling experimental evidence for bioconvection in a natural water body (the alpine Lake Cadagno in Switzerland) induced by the 10-μm-long, motile, purple bacterium *Chromatium okenii*. These bacteria gain energy from light-driven sulphide oxidation. High cell concentrations were observed in 30- to 120-cm-thick mixed layers of uniform temperature and salinity 12 m below the surface, in deep regions that are otherwise meromictic (monotonically increasing density with depth). The bacteria were found to be 15–27% denser than water with swimming speeds of 27 μm/s. Simulations of upward-swimming cells exclusively below an imposed oxycline (a sharp gradient in oxygen concentration) led to cell accumulation and instability. The authors found that bioconvection with *C. okenii* was sufficient to explain the observed mixed layer. They indicated that the mean theoretical dissipation rate in the layer was $1.0 \pm 1.5 \times 10^{-10}$ W/kg, or 45% of the bacterial energy input rate, matching in situ measurements. The authors suggest that bioconvection is widespread in regions of lakes where turbulence is relatively weak.

3. MODEL FORMULATION

In most studies of bioconvection, the aim is to describe the macroscale phenomena at a continuum level using information about the microscopic behavior of individual organisms. As discussed earlier, bioconvection sits mainly at the dilute end of the cell concentration spectrum, and so direct cell–cell interactions are mostly neglected. The main constituents of the standard continuum approach are momentum balance, mass balance, cell conservation, and a description of cell orientation moments as a function of the flow.

Typically, the individual cell Reynolds number is small (e.g., $\sim 10^{-3}$ for *C. augustae*) relative to the bioconvection Reynolds number (e.g., ~10). The general model is based on the incompressible Navier–Stokes equations with an added (negative) buoyancy term (Childress et al. 1975,

Pedley & Kessler 1990) (subject to a Boussinesq approximation) that represents the main effect of the difference in density between the cell and fluid, $\Delta\rho$, for cells of concentration $n(\mathbf{x},t)$ and mean volume v. Typically, the cells are a little more dense than the fluid (e.g., *C. augustae* are 5% more dense than the fluid). Additionally, the presence of the swimming cells may impact the bulk stress, $\Sigma(\mathbf{x},t)$. Hence, we obtain

$$\rho\frac{\mathrm{D}\mathbf{u}}{\mathrm{D}t} = -\nabla p_\mathrm{e} + nv\Delta\rho\mathbf{g} + \nabla\cdot\Sigma, \quad \nabla\cdot\mathbf{u} = 0, \qquad 1.$$

where $\mathbf{u}(\mathbf{x},t)$ represents the velocity of the suspension, $n(\mathbf{x},t)$ is the cell concentration, $p_\mathrm{e}(\mathbf{x},t)$ is the excess pressure, ρ is the fluid density, and $\mathbf{g}$ is the gravitational acceleration. Pedley & Kessler (1990) were the first to consider cell-induced stresses in Σ. They identified three components: swimming-induced stresslets, Batchelor stresses, and stress associated with rotary particle diffusion. It was found that the last two of these could be neglected (with no new qualitative features from the Batchelor stresses and the same tensorial form for the rotary particle diffusion stress as for the swimming stresslets). However, the first term, the leading-order stress for the aggregate swimming stroke of the cells, $\Sigma^{(p)}$, has been found to play a significant role in concentrated suspensions (Pedley 2010). Thus, we may write $\nabla\cdot\Sigma = \mu\nabla^2\mathbf{u} + \nabla\cdot\Sigma^{(p)}$, where μ is the fluid viscosity (see Section 4.4).

The timescale for bioconvection is much shorter than for cell growth. Therefore, a cell conservation equation of the form

$$\frac{\partial n}{\partial t} = -\nabla\cdot\mathcal{J}, \quad \text{with flux } \mathcal{J} = [n(\mathbf{u}+\mathbf{V}_\mathrm{c}) - \mathsf{D}\cdot\nabla n], \qquad 2.$$

was proposed (Pedley et al. 1988, Pedley & Kessler 1990), where the flux terms represent advection by the flow $\mathbf{u}$, drift relative to the flow with mean swimming velocity $\mathbf{V}_\mathrm{c}(\mathbf{x},t)$, and swimming diffusion with diffusion tensor $\mathsf{D}(\mathbf{x},t)$. These last two terms, together with $\Sigma^{(p)}$, are functions of the swimming behavior and need to be specified. Descriptions for individuals are either phenomenological or derived from external torques coupled to low–Reynolds number fluid mechanics. Appropriate forms of $\mathbf{V}_\mathrm{c}(\mathbf{x},t)$ and $\mathsf{D}(\mathbf{x},t)$ for each taxis are described in the sections below. Under certain conditions, Equation 2 can be established directly by approximating a Smoluchowski equation (Hill & Bees 2002, Manela & Frankel 2003, Hwang & Pedley 2014a) for the probability that a cell has a particular position and orientation (Section 4.2).

Initial conditions generally specify a fully mixed suspension or a steady, horizontally uniform, vertical profile. For stationary boundaries $\mathcal{B}$ with unit normal $\mathbf{n}_\mathcal{B}$, a kinematic condition imposes $u_\mathrm{n} := \mathbf{u}\cdot\mathbf{n}_\mathcal{B} = 0$, and we have a choice of no-slip, $\mathbf{u}_\mathrm{t} := \mathbf{u} - u_\mathrm{n}\mathbf{n}_\mathcal{B} = \mathbf{0}$, or stress-free, $\mathbf{n}_\mathcal{B}\cdot\nabla\mathbf{u}_\mathrm{t} = \mathbf{0}$, conditions on $\mathcal{B}$ together with zero cell flux normal to $\mathcal{B}$, such that $\mathbf{n}_\mathcal{B}\cdot\mathcal{J} = 0$ on $\mathcal{B}$.

Models for bioconvection have been highly successful, describing pattern formation with remarkable agreement between experiment and theory. A huge part of this success is that there are very few parameters that cannot be measured; observations of individuals can generally parameterize the system without resorting to fitting.

4. GYROTACTIC BIOCONVECTION

4.1. Bottom Heaviness Versus Sedimentation Torque

The mechanisms responsible for gravitaxis may be active or passive. Results of experiments in micro- and hypergravity with the ciliate *Euglena* have suggested the existence of a gravity receptor (Häder et al. 2005). However, the nature of the receptor remains unclear, and in many cases, passive mechanisms appear sufficient to explain experimental observations. Two mechanisms have been

identified for passive gravitaxis: bottom heaviness (center of mass below the center of buoyancy, sometimes called a gravity-buoyancy mechanism) (Kessler 1986) and a sedimentation torque due to body asymmetry (Roberts 1970). Recent experiments in a hyperdense medium (using Percoll) found that the principal mechanism for gravitaxis in *Paramecium caudatum* is due to geometrical asymmetry of the sedimenting cell (Mogami et al. 2001), as supported by scale models (Roberts & Deacon 2002), whereas sea urchin larvae switch between the two mechanisms for gravitaxis as they develop (Mogami et al. 2001).

Hill & Häder (1997) and Vladimirov et al. (2004) tracked individual cells (*Chlamydomonas*) and found that under conditions of no flow, cells execute a random walk with a swimming speed distribution and a well-defined gravitactic bias. As they swim, these biflagellates perform a back-and-forth flagella beat. Recently, a fast, high-throughput method called differential dynamic microscopy was developed (Martinez et al. 2012, Croze et al. 2019) to parameterize such detailed flagellar beats and motion in three dimensions (fitting the intermediate scattering function from spatiotemporal fluctuations of the intensity with low-magnification microscopy and obtaining distributions for 10^4 cells in minutes).

Normally, gravitactic cells swim upward on average under quiescent conditions. As cells typically are more dense than the fluid in which they swim, cell accumulation at an upper boundary can drive an overturning instability. However, Kessler (1984) realized that a combination of gravitational and viscous torques can tip cells on average from the vertical so that they swim toward locally downwelling flow (e.g., toward the center of downwelling Poiseuille flow in a vertical tube). He termed this directed motion gyrotaxis. Furthermore, a gyrotactic instability can arise in the absence of an upper boundary as cells swim toward downwelling regions, causing these regions to sink more quickly. **Figure 4*a–g*** presents various experiments displaying evidence of gyrotaxis and gyrotactic instabilities.

O'Malley & Bees (2012) investigated gyrotaxis for the biflagellate *C. reinhardtii* using a computational approach [the method of regularized Stokeslets (Cortez et al. 2005)], extending an earlier study that used resistive force theory (Jones et al. 1994). In particular, they explored the impact of distinct time-dependent flagella beat patterns (**Figure 3*a***) on the fluid dynamics and contrasted the two competing passive gravitational reorientation mechanisms, bottom heaviness and sedimentation, in linear shear flow. The body of the microorganism (∼10 μm long) is prolate spheroidal and contains a cup-shaped posterior chloroplast that is thought to be responsible in part for the measured bottom heaviness (Kessler 1986). The microorganisms have two anterior flagella that they beat at 50 Hz in a breaststroke fashion to propel themselves forward at several body lengths per second. While translation due to sedimentation is a small fraction of the swimming speed and can be neglected, the body sediments more quickly than the flagella, leading to a sedimentary torque (Roberts 1970) that is comparable in size to the gravitational torque due to bottom heaviness. With the most realistic flagella beat patterns taken from experimental observations, O'Malley & Bees (2012) found that both gravitational reorientation mechanisms were equally important and that changes to the beat pattern tended to be complementary. In other words, an increase in flagellar extension from the body can increase the sedimentation torque but also reduces the gravitational-to-viscous torque ratio associated with bottom heaviness. O'Malley & Bees (2012) placed their model swimmer with a time-dependent flagellar beat into a constant linear shear flow and fitted the beat-averaged orientation dynamics to an exact equation for the reorientation of a spheroid. They found that the two mechanisms can be combined into a simple gyrotactic torque balance and were able to measure the effective gravitational torque parameter and effective cell eccentricity from the fitting process. Surprisingly, the magnitude of the effective cell eccentricity in the plane of the beating flagella was much smaller (approximately zero) than for the body alone due to the extended periods where the flagella lie lateral to the body. Notably, the precise swimming stroke matters:

The swimming stroke alters the effective cell eccentricity, with the potential for qualitative changes of swimming trajectories in shear flows in response to environmental conditions.

4.2. Scaling Up

Early descriptions of gyrotaxis were deterministic (Pedley & Kessler 1987). For a small microorganism Reynolds number, a torque balance suggests that the orientation $\mathbf{p}$ of a spheroidal swimming cell is governed by

$$\dot{\mathbf{p}} = \frac{1}{2B}[\mathbf{k} - (\mathbf{k}\cdot\mathbf{p})\mathbf{p}] + \frac{1}{2}\boldsymbol{\Omega}\times\mathbf{p} + \alpha_0[\mathsf{E}\cdot\mathbf{p} - \mathbf{p}\mathbf{p}\cdot\mathsf{E}\cdot\mathbf{p}], \qquad 3.$$

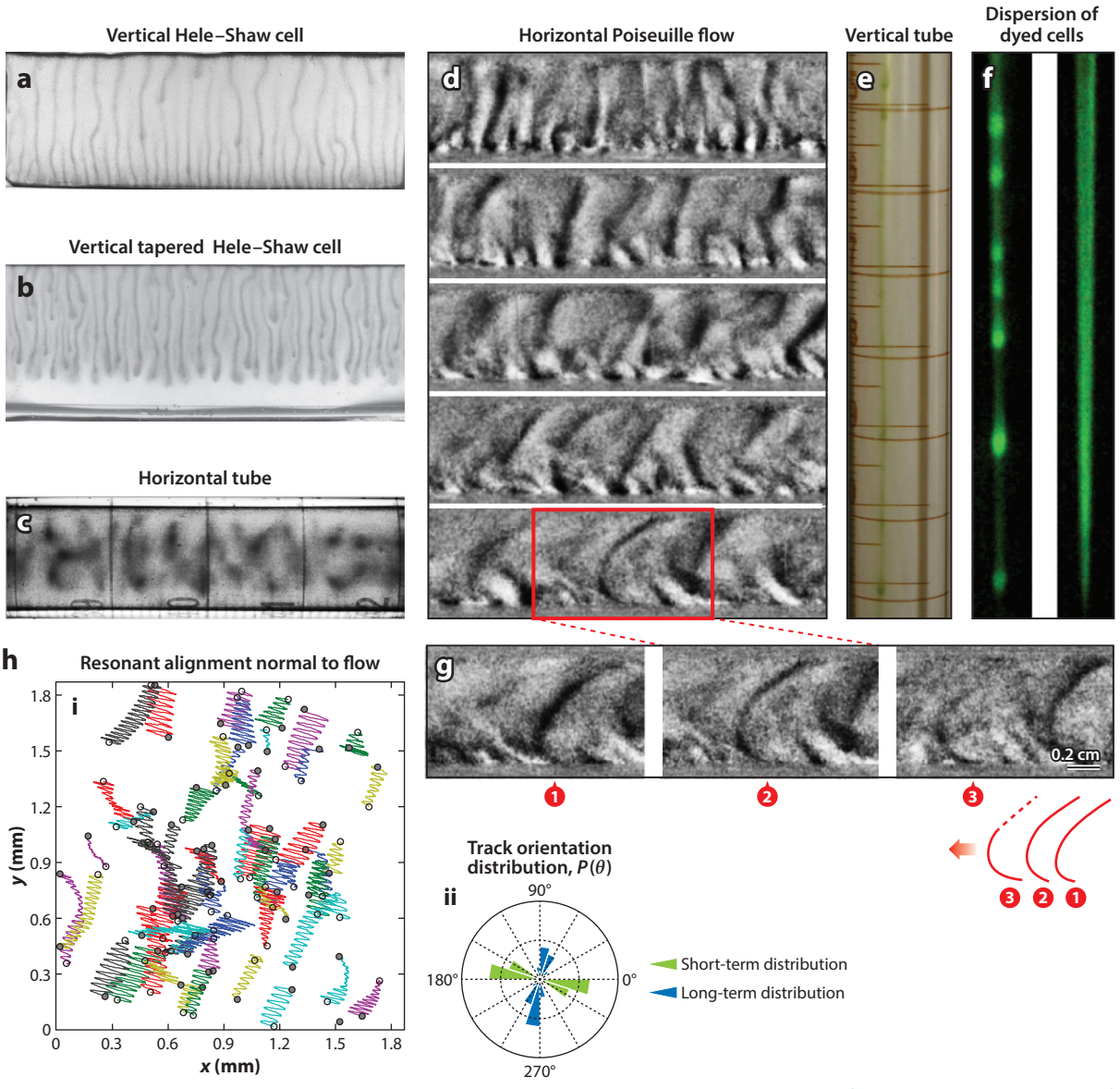

(*Caption appears on following page*)

Figure 4 (*Figure appears on preceding page*)

Bioconvection patterns in Hele–Shaw cells and with flow in suspensions of *Chlamydomonas augustae*, except for panels *f* and *h*, which are *Dunaliella salina*. (*a*) Bioconvection plumes from the side in a vertical Hele–Shaw cell between two glass slides (10^6 cells/cm^3, with a channel width of 1 mm and height of 2.5 cm). Bottom-standing plumes are evident with a much smaller wavelength than at the top. (*b*) Same as panel *a* except for a tapered vessel (1 mm wide at the top and touching at the bottom). Gyrotactic instabilities occur in the top third of the vessel, and plumes propagate downward but slow sufficiently for the cells to swim out of the plume head. No cells are observed in the lower quarter of the vessel even though it is an order of magnitude wider than a cell. (*c*) Bioconvection seen from above in a horizontal tube of diameter 2 cm. (*d*) Bioconvection plumes in Poiseuille flow, with a mean speed of 8.3×10^{-3} cm/s, in a horizontal tube of diameter 2 cm (2.2×10^6 cells/cm^3). (*e*) Gyrotactic plume in an almost vertical cylinder of diameter 2 cm displaying a secondary blip instability (10^5 cells/cm^3). (*f*) Fluorescently labeled slugs of *D. salina* dispersing in pipe flow. (*g*) Propagation of a bioconvection plume from panel *d*. The plume is seen to travel to the left, as characterized in the sketch, roughly maintaining its shape in the imposed shear but not cell concentration. (*h*) Resonant alignment tracks of helically swimming cells in an oscillatory shear flow (2 Hz, with an amplitude of 440 μm and depth of 400 μm). (*i*) Tracks of swimming cells, illustrating the alignment of long-term tracks of cells perpendicular to the shear plane. (*ii*) The track orientation distribution, $P(\theta)$; green is the short-term distribution, matching the oscillatory flow direction, and blue is the long-term distribution. Panels adapted or reprinted with permission from (*a*,*e*) Bees & Croze (2014), (*c*,*d*,*g*) Croze et al. (2010), (*f*) Croze et al. (2017), and (*h*) Hope et al. (2016). Panel *a* and *b* photos courtesy of M.A. Bees and J.O. Kessler.

where $B = \mu\alpha_\perp/2h\rho g$ is the gyrotactic reorientation timescale, $\mathbf{k}$ is the vertically upward unit vector, h is the center-of-mass offset, $\alpha_\perp$ is the dimensionless resistance coefficient, and $\alpha_0 = (a^2 - b^2)/(a^2 + b^2)$ measures cell eccentricity (a and b are semimajor and semiminor axes; $\alpha_0 = 0$ for a sphere). The first term is the gravitational torque, the second and third are the torques due to vorticity, $\mathbf{\Omega} = \nabla_\mathbf{R} \times \mathbf{u}$, and the rate-of-strain, $\mathsf{E} = \frac{1}{2}\left[\mathsf{G}^\mathrm{T} + \mathsf{G}\right]$, where $\nabla_\mathbf{R}$ is the spatial gradient operator and $\mathsf{G} = (\nabla_\mathbf{R}\mathbf{u})^\mathrm{T}$ is the (transpose of the) fluid velocity gradient. The mean swimming velocity is then given by $\mathbf{V}_\mathrm{c} = V_\mathrm{s}\mathbf{p}$, where V_s is the mean swimming speed. Additionally, the diffusion tensor is assumed to be orthotropic.

Pedley & Kessler (1990) reasoned that such a treatment is inconsistent in that swimming orientation is assumed to be deterministic, yet the swimming diffusion term, which is used to account for observed variations in cell swimming stroke and trajectory, is set independent of gyrotaxis. Thus, they employed a Fokker–Planck equation for $f(\mathbf{p})$, the probability density of swimming orientations at a point, as a function of fluid velocity gradients, of the form

$$\frac{\partial f}{\partial t} + d_\mathrm{r}\mathcal{L}f = 0, \qquad 4.$$

where the linear operator $\mathcal{L}$ is defined by $\mathcal{L}f = \nabla_\mathbf{p} \cdot \left[d_\mathrm{r}^{-1}\dot{\mathbf{p}}f - \nabla_\mathbf{p}f\right]$; d_r is rotational diffusivity, modeling randomness in cell orientation due to biological variation in motility; and $\nabla_\mathbf{p}$ is the orientational gradient operator. The mean swimming direction,

$$\mathbf{q} \equiv \langle\mathbf{p}\rangle = \int_{S_2} \mathbf{p}f(\mathbf{p})\,\mathrm{d}^2\mathbf{p}, \qquad 5.$$

can be calculated directly, where S_2 is the surface of the unit sphere, yielding the mean velocity $\mathbf{V}_\mathrm{c} = V_\mathrm{s}\mathbf{q}$. However, as only the cell orientation distribution is known, the physical-space cell swimming diffusion tensor needs to be approximated. Pedley & Kessler (1990) proposed $\mathsf{D} = V_\mathrm{s}^2\tau\,\mathrm{var}(\mathbf{p})$, where τ is a direction correlation time, to be estimated from experimental data. Using a Galerkin method, Bees et al. (1998) expanded the Fokker–Planck equation in spherical harmonics to find the mean orientation and diffusion tensor for all flow gradients. For simplicity, quasi-steady and quasi-uniform solutions (where f evolves slowly in time and space; typically $\tau \sim 1.3$–5 s) are often assumed and the Pedley & Kessler diffusion approximation, $\mathsf{D} = V_\mathrm{s}^2\tau\,\mathrm{var}(\mathbf{p})$, is commonly used (Bees & Hill 1998, Hwang & Pedley 2014b, Pedley 2015), resulting in a system equivalent to that of Pedley & Kessler (1990).

However, uncertainty over the validity of the diffusion approximation, particularly for large shear rates, led Hill & Bees (2002) and Manela & Frankel (2003) to formulate generalized Taylor dispersion theory for biased swimming cells. The theory starts with the Smoluchowski equation,

$$\frac{\partial P}{\partial t} + \nabla_{\mathbf{R}} \cdot \mathbf{J} + \nabla_{\mathbf{p}} \cdot \mathbf{j} = 0, \tag{6.}$$

with physical-space and orientational-space probability flux densities

$$\mathbf{J} = \left[\mathbf{u}(\mathbf{R}) + V_c \mathbf{p}\right] P \quad \text{and} \quad \mathbf{j} = \dot{\mathbf{p}} P - d_r \nabla_{\mathbf{p}} P, \tag{7.}$$

respectively. Here, $P(\mathbf{R}, \mathbf{p}, t|\mathbf{R}', \mathbf{p}')$ is the probability of finding a swimming cell at position $\mathbf{R}$ with orientation $\mathbf{p}$ at time t_0, given initial primed data. The method develops spatial moments to derive the leading-order, long-time spatial diffusion tensor for the physical-space variable $\overline{P}(\mathbf{R}, t|\mathbf{R}', \mathbf{p}') \equiv \int_{S_2} P(\mathbf{R}, \mathbf{p}, t|\mathbf{R}', \mathbf{p}')\, \mathrm{d}^2\mathbf{p}$.

For a linear flow $\mathbf{u}(\mathbf{R}) = \mathbf{u}(\mathbf{R}') + (\mathbf{R} - \mathbf{R}') \cdot \mathsf{G}$, Hill & Bees (2002) showed that the leading-order long-time ($t \gg d_r^{-1}$) asymptotic behavior of $\overline{P}$ is given by the solution of

$$\frac{\partial \overline{P}}{\partial t} + \nabla_{\mathbf{R}} \cdot \left[\left(\mathbf{u} + \overline{\mathbf{U}}\right) \overline{P} - \overline{\mathsf{D}} \cdot \nabla_{\mathbf{R}} \overline{P}\right] = 0, \tag{8.}$$

provided that the eigenvalues of G are purely imaginary so that advection alone does not cause exponential divergence in physical space. The quantities $\overline{\mathbf{U}}$ and $\overline{\mathsf{D}}$ that appear in Equation 8 represent a drift velocity and effective swimming diffusion tensor for the cells and are computed using generalized Taylor dispersion theory in terms of spatial moments. The upshot is that $\overline{P}$ is identified with n, $\overline{\mathbf{U}}$ turns out to be given by $V_s\mathbf{q}$ from Equation 5, where $f(\mathbf{p})$ satisfies $\mathcal{L}f = 0$, subject to $\int_{S_2} f\, \mathrm{d}^2\mathbf{p} = 1$, and the diffusion tensor is

$$\overline{\mathsf{D}} = \frac{V_s^2}{d_r} \int_{S_2} \left[\mathbf{bp} + \frac{2\sigma}{f(\mathbf{p})} \mathbf{bb} \cdot \hat{\mathsf{G}}\right]^{\mathrm{sym}} \mathrm{d}^2\mathbf{p}. \tag{9.}$$

Here $[\cdot]^{\mathrm{sym}}$ denotes the symmetric part of the tensor argument, σ is the dimensionless shear rate, $\hat{\mathsf{G}}$ is nondimensional G, and $\mathbf{b}(\mathbf{p})$ satisfies

$$\mathcal{L}\mathbf{b} - 2\sigma \mathbf{b} \cdot \hat{\mathsf{G}} = f(\mathbf{p})(\mathbf{p} - \mathbf{q}), \tag{10.}$$

subject to a normalization condition $\int_{S_2} \mathbf{b}\, \mathrm{d}^2\mathbf{p} = 0$ (Hill & Bees 2002). The techniques were subsequently employed by Bearon (2003) for dispersion of chemotactic bacteria in a shear flow.

Bearon et al. (2012) provided compact expressions for components of the mean swimming direction and the diffusion tensor for the gyrotactic problem with simple expressions of the form $\left(a_0 + a_2\sigma^2 + a_4\sigma^4\right) / \left(1 + b_2\sigma^2 + b_4\sigma^4\right)$, where the constants a_0, a_2, a_4, b_2, and b_4 are determined to match asymptotic solutions, for both the orientation-only Fokker–Planck model (the F model) and the generalized Taylor dispersion model (the G model). However, if the eigenvalues of G are not purely imaginary, then the theory formally breaks down and the advection–swimming–diffusion equation is suspect. One should question whether it fails in significant regions of a flow. Recently, in simulations Bearon et al. (2011) found that the Hill & Bees (2002) result describes the transport of cells mostly well except in the vicinity of stagnation points.

Notably, the diffusivity of biased swimming cells is qualitatively different for the F and G models for large vorticity. In essence, as vorticity increases beyond a threshold, the cells tumble, and in a plane normal to the vorticity vector, their orientations scan all directions, yielding in the F model in the limit of large vorticity $\mathsf{D} \propto \mathrm{var}(\mathbf{p})$ with three nonzero eigenvalues. However, the G model explicitly evaluates the spatial moments: As vorticity increases, the tumbling cells swim in

tighter trajectories and sample less of the shear flow; components of the diffusion tensor normal to the vorticity decay to zero with increasing vorticity.

4.3. Testing the Theory: Dispersion in Tubes

With competing descriptions and qualitatively different predictions, it is necessary to establish a test to determine which description is best suited for suspensions of swimming cells in shear. Bees & Croze (2010) considered the dispersion of cells in a vertical tube. Flow was either generated by an imposed pressure gradient or induced by the accumulation of negatively buoyant gyrotactic cells. They used axial moments to calculate drift and effective diffusivity and found that, unlike normal Taylor dispersion, cells drift axially relative to the mean flow. General expressions for any taxis were provided for the drift, effective diffusivity, and skewness of the distributions, and their limits were explored. Bearon et al. (2011) extended the results in channels to directly compare the F and G models: Qualitative differences in the nonmontonic drift and diffusion with Péclet number were predicted. Simulations of swimming gyrotactic cells in laminar and turbulent flow in a channel found excellent agreement with the G model; the F model differed qualitatively (see Croze et al. 2013, figure 12). Recently, Croze et al. (2017) conducted experiments with a suspension of the gyrotactic alga *D. salina* in long vertical tubes with a pressure gradient (see **Figure 4*f***). To avoid generating local bioconvective circulation, fluorescently stained cells were introduced into existing plume structures and the drift of the stained blob monitored. Good agreement was found between the experimental results and predictions from the G model; poor agreement was found with the F model (Croze et al. 2017, figure 4). The conclusion is clear: The F model (based on the Fokker–Planck equation for orientation alone) is qualitatively incorrect for anything other than small shear rates, whereas the G model (employing generalized Taylor dispersion) is consistent with linear shear experiments for all shear rates.

The blip features observed in **Figure 4*e*,*f*** have been investigated experimentally (Denissenko & Lukaschuk 2007) and theoretically (Ghorai & Singh 2009, Hwang & Pedley 2014b). Notably, the steady plume solutions are subject to a varicose instability that has been found to be due principally to the horizontal gradient in cell orientation from nonuniform shear in alliance with the gyrotactic instability.

4.4. Semidilute Suspensions

Pedley (2010) reconsidered his earlier analysis of gyrotactic instabilities in uniform suspensions (Pedley & Kessler 1990) in light of the active matter analysis for instabilities in concentrated suspensions of interacting swimming cells, first recognized by Simha & Ramaswamy (2002) but explored by many others (Ramaswamy 2010). Pedley & Kessler (1990) formulated the stresslet contribution to the bulk stress tensor due to identical swimming cells of concentration n, which takes the form

$$\boldsymbol{\Sigma}^{(p)} = nS\left(\langle \mathbf{pp} \rangle - \frac{1}{3}\mathsf{I}\right), \qquad 11.$$

where, as before, the angled brackets represent an average over orientation space, and S is the strength of the swimming stresslet ($S > 0$ for pullers and $S < 0$ for pushers). Using a Smoluchowski equation for the distribution of swimming cells (comparable with Equation 6), Pedley (2010) averaged over orientation space and, with some additional assumptions about the size of terms, constructed the orientation-only Fokker-Planck description and cell conservation equation. Additionally, the diffusion approximation of Pedley & Kessler (1990) based on the variance of $\mathbf{p}$ was simplified further for convenience. This allowed for the study of stresslet-induced

instabilities. Notably, Pedley (2010) did not use a quasi-steady assumption for the distribution of cell orientations, $f(\mathbf{p})$, and because of this it was found that S must exceed a critical value, depending on viscosity and rotational diffusivity, for a stresslet-induced instability, in contrast to Simha & Ramaswamy (2002), who observed instability for all S. Also noted is the possibility of instability in swimming direction coupled to nonzero fluid inertia (a mode that is expected to be quashed by viscosity).

An alternative approach is to consider detailed numerical models of individuals and scale up by considering interactions of many cells (Ishikawa 2009). An example is the Stokesian dynamics of interacting squirmer cells (Ishikawa & Pedley 2014), which can provide insights into instability mechanisms and useful measures of dispersion.

4.5. Bioconvection in Shear Flow

Bioconvection patterns observed in a horizontal tube (diameter 2 cm) are presented in **Figure 4*c*,*d*,*g***. In **Figure 4*c*** and at the top of **Figure 4*d*** there is no flow. An imposed pressure-driven pipe flow reveals deformation of the plume structures in **Figure 4*d*** (flow is from right to left; flow velocity increases from top to bottom) eventually leading to their demise if shear is sufficiently large (Croze et al. 2010). This study motivated Hwang & Pedley (2014a) to investigate the effects of shear on bioconvection in a shallow suspension. The system is reminiscent of Rayleigh–Bénard convection in shear, but the behaviors of the systems differ markedly, particularly as the base state of the latter is not modified by the flow, unlike bioconvection. In particular, they followed Pedley (2010) in constructing cell conservation and orientation-only Fokker–Planck equations, included sedimentation but neglected swimming stresslets (a dilute system), and imposed a shear flow. To make progress, they assumed the cell orientation distribution is quasi-steady and quasi-uniform. They also used the Pedley & Kessler (1990) approximation for the swimming diffusion tensor, $\mathsf{D} = V_s^2 \tau\, (\langle \mathbf{pp} \rangle - \mathbf{qq})$, which strictly is valid only for small shear. With no shear, Hwang & Pedley (2014a) pointed out that in addition to the easily visualized gravitational overturning and gyrotactic instabilities (**Figure 2**), there is a third instability mechanism in a shallow layer (documented but not discussed by Bees & Hill 1998) associated with a negative cross-diffusion in a positive vertical concentration gradient: Near the upper boundary the diffusive flux is horizontal, from less to more concentrated regions, driving an instability. Saintillan (2014) has questioned the robustness of the mechanism in that it depends on the precise formulation of the diffusion tensor. However, both the Pedley & Kessler (1990) approximation (see Bees et al. 1998) and the generalized Taylor dispersion theory (G model) (Hill & Bees 2002, Bearon et al. 2012) have negative cross-diffusion, the latter being specifically designed for all values of the shear rate. For weak shear, perturbations of the system with small wave number are destabilized, whereas large–wave number perturbations are stabilized, mainly due to the overturning instability for a modified base state and weakened gyrotaxis, respectively. The modes of instability become tilted, in good agreement with experiments (Croze et al. 2010). For large shear, upward-swimming motion is inhibited because the cells tend to tumble and must compete with sedimentation, thereby stabilizing the system fully for sufficiently high shear rate. However, beyond small shear rates, the use of the diffusion approximation via the F model is qualitatively questionable (see Section 4.2), and the analysis should be repeated with the G model.

Helical motion is intrinsic to many swimmers. Bearon (2013) developed a model of a helical gyrotactic swimmer, based on the HAB species *H. akashiwo*, to explore whether upward swimming was robust in shear flows. In particular, the torque balance for a spherical swimmer was modified to $\mathbf{\Omega} = G\mathbf{p} \times \mathbf{k} + R\mathbf{n} + \frac{1}{2}\boldsymbol{\omega}$, where $R\mathbf{n}$ is an intrinsic torque in direction $\mathbf{n}$, different from the swimming direction $\mathbf{p}$ subject to the constraint $\mathbf{p} \cdot \mathbf{n} = \cos\gamma$ for constant angle γ. This description

results in helical motion. As both $\mathbf{n}$ and $\mathbf{p}$ are unit vectors, they must satisfy $\dot{\mathbf{p}} = \boldsymbol{\Omega} \times \mathbf{p}$ and $\dot{\mathbf{n}} = \boldsymbol{\Omega} \times \mathbf{n}$, which provides a dynamical system with three degrees of freedom. Bearon (2013) found that downward transport is suppressed for helical swimmers in vertical shear flow, leading mostly to robust upward transport. In downwelling channel flow gyrotactic focusing is preserved, but a new phenomenon was discovered where for a range of parameters cells focus away from the centerline (Alqarni & Bearon 2016). Helical motion can also give rise to some unexpected results in oscillatory shear flows (**Figure 4*b***). In particular, resonance effects can arise if the frequency of oscillation, shear rate, and helical frequency (typically 2 Hz for *C. augustae*) are commensurate, leading cells to make progress only in a direction perpendicular to the shear plane (Hope et al. 2016). It remains to be seen what effects helical motion has on bioconvection in shear.

4.6. Numerical Treatment of Gyrotactic Bioconvection

Linear analysis has its place in predicting when suspensions will be unstable to patterns and flow. There have been some useful comparisons between theory and experiments (Bees & Hill 1998) that predict the correct qualitative behavior but tend to either overestimate [deterministic gyrotaxis (Hill et al. 1989)] or underestimate [orientation only; Fokker–Planck (Bees & Hill 1998)] observed initial pattern wavelengths (Bees & Hill 1997), using directly measured parameter values. Beyond analytical nonlinear techniques for particular solutions (Bees & Hill 1999), one can use numerical approaches to access the full wealth of solution behavior. Early numerical studies are described by Hill & Pedley (2005): Aspects of gyrotactic bioconvection are explored in various geometries, notably including periodic arrays in 2D (Ghorai & Hill 2000), varicose instabilities in axisymmetric solutions (Ghorai & Hill 2002), and a 2D combined Eulerian–Lagrangian approach (Hopkins & Fauci 2002). More recently, fully 3D simulations have revealed the presence of varicose instabilities, but in deep chambers plumes typically are destabilized by meandering modes (Ghorai & Hill 2007), conclusions that are qualitatively similar to the 2D simulations. Karimi & Paul (2013) explored 3D dynamics in larger systems, and most recently, Ghorai et al. (2015) found good agreement of predicted pattern wavelengths with experiments together with elusive computational evidence of bottom-standing plumes.

4.7. Implications of Gyrotaxis and Cell Elongation

There are many proposed applications of gyrotaxis where cells are driven by flow gradients but do not necessarily generate bioconvection flows [e.g., gyrotactic cells in turbulence (Lewis 2003, Thorn & Bearon 2010) and bubble plumes (Nonaka et al. 2016)]. Durham et al. (2009) proposed that horizontal shear flows can trap gyrotactic cells in regions where the shear rate exceeds that for the cells to tumble, potentially explaining observations of thin phytoplankton layers in the oceans, motivating other studies (Thorn & Bearon 2010, Hoecker-Martinez & Smyth 2012, Durham et al. 2013, Santamaria et al. 2014, Ghorai 2016, Richardson et al. 2018). In a vertically aligned cylindrical water vessel in solid body rotation, Cencini et al. (2016) found that *C. augustae* tended to swim toward and accumulate close to the axis. They explained these observations by replacing the gravitational torque in an orientation-only Fokker–Planck description of gyrotaxis by that due to gravity plus rotational acceleration. Their analytical and numerical solutions were in quantitative agreement with experiments. With the development of a reinforcement learning algorithm, Colabrese et al. (2017) demonstrated how smart gyrotactic swimmers learn effective strategies (by shifting their preferred swimming direction from the vertical) to escape from situations where they would normally be trapped by flow structures.

Swimming nongyrotactic elongated cells exhibit convoluted trajectories in prescribed pressure-driven flows, simply due to the coupling of viscous torques and translation in

position-dependent shear (Zöttl & Stark 2013). Additional effects can lead to mean drift relative to flow in tubes (Mathijssen et al. 2016).

In a similar vein, even nonswimming but sedimenting spheroidal cells are of interest in turbulent (Ardekani et al. 2017) or even simple shear flows (Clifton et al. 2018), displaying some remarkably complex dynamics, with cells aligning with shear flow and spending more time in faster-moving downwelling regions. The chirality of the microorganism may also be implicated in cell accumulation. Marcos et al. (2009) observed drift across streamlines of nonswimming, helical spirochete bacteria in shear flow; the mechanism is due to coupling between cell chirality and flow alignment via Jeffery orbits.

5. PHOTOTACTIC BIOCONVECTION

Phototaxis can drive or disrupt the formation of bioconvection patterns (**Figure 5*a***). Vincent & Hill (1996) constructed and analyzed the first model of purely phototactic bioconvection. Equations 1 and 2 were used with swimming velocity given by $\mathbf{V}_c = V_s\mathbf{q} = V_sT(I)\mathbf{k}$, where the phenomenological taxis function $T(I)$ was positive if the light intensity $I(x,t)$ was less than the critical light intensity I_c and negative otherwise (typically nonlinear, but with a linear response with negative gradient near I_c). The diffusion tensor was assumed constant and orthotropic. The well-known Lambert–Beer law was employed to model the absorption of incident light from above the cells in suspension such that $I(\mathbf{x},t) = I_s \exp\left[-\alpha \int_{z<0}^{0} n(\mathbf{x},t)\,dz\right]$, where I_s is the light intensity at the surface $z = 0$ and α is the absorption coefficient. The no-flow base state about which the stability is assessed can vary qualitatively: Cells accumulate at the top if the light is weak, at the bottom if the light is strong, or within a peak for a narrow range of intermediate light intensities. The first case is somewhat like gravitactic bioconvection, the second is stable, and the third can generate bioconvective flows from the unstably stratified suspension in the lower region that can penetrate into the stable upper region, called penetrative bioconvection. As with similar systems, oscillatory solutions are possible. An error was corrected and the solution behavior was explored numerically by Ghorai & Hill (2005) (for lateral walls, see Panda et al. 2016). However, the Vincent & Hill (1996) description neglects (*a*) the biology and mechanisms of phototaxis, (*b*) viscous and gravitational torques, and (*c*) representation of the physics of scattering by the microorganisms.

Many organisms such as *Chlamydomonas* or *Euglena* possess a photoreceptor that is shielded in some way from other directions and swim with a helical trajectory. For example, *Chlamydomonas* have a layered stack of chloroplast membranes with carotenoid granules that reflect photons back to overlying photoreceptors, shielding other directions. As the cell rotates (e.g., 2 Hz) the photoreceptor receives a light signal that it converts into individual flagellar responses (via Ca^{2+} signaling), leading the cell to turn toward or away from the light source (e.g., Bennett & Golestanian 2015).

An open question is how this individual behavior should be converted into a continuum description. Seeking to generalize for a range of microorganisms, Williams & Bees (2011a) proposed three distinct mechanisms for the light response of individuals, all within the Pedley & Kessler (1990) Fokker–Planck framework. The first is photokinesis, a change in swimming speed in response to light intensity, $V_s = V_s(I)$, with a similar form to $T(I)$. The second concerns mechanical properties of the cell. With the sedimentation torque in mind, it is conceivable that cells could alter their flagellar stroke or body shape in response to light and so adjust the gravitational reorientation mechanism or, equivalently, the effective center-of-mass offset. Hence, they set $B = B(I)$, with a response such that normal gyrotaxis is recovered in the dark. The third mechanism proposed was an additional phototactic torque, a function of I or ∇I, of the form

$$\mathbf{L}_p = f(I)\mathbf{p} \times (\beta_1\boldsymbol{\pi} + \beta_2\nabla I),$$

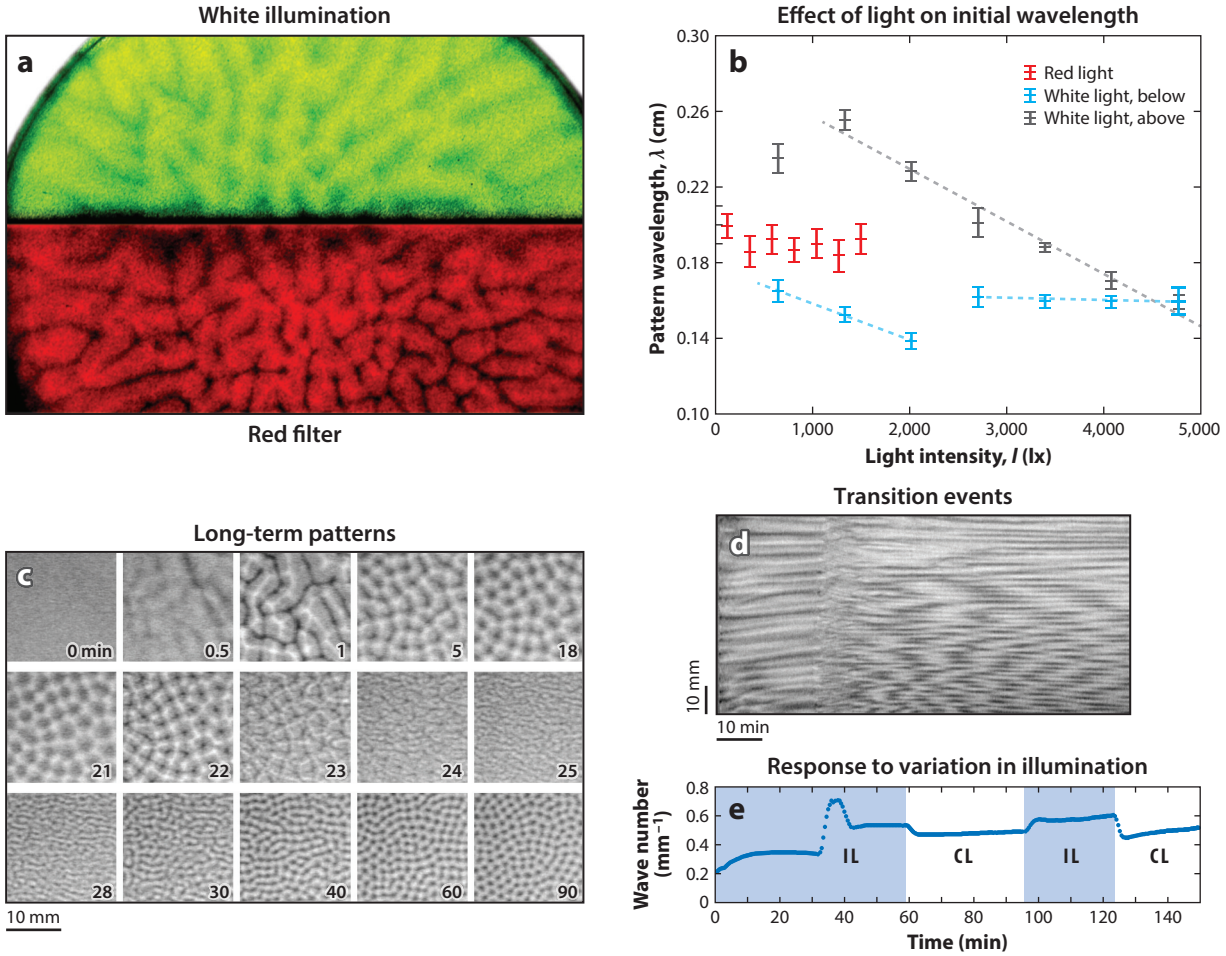

Figure 5

(*a*) Phototactic bioconvection in *Chlamydomonas augustae* (10^6 cells/cm^3, with a depth of 0.4 cm and a width of 5 cm). White illumination (*top*) leads cells to swim upward, with phototaxis supporting gravitaxis and suppressing gyrotaxis, initiating an overturning instability with broad downwelling structures; with a red filter (660 nm; *bottom*), cells do not respond to illumination and form focused connected gyrotactic plumes. (*b*) Effect of light intensity, color, and position on initial bioconvection pattern wavelength, λ, for suspensions of *C. augustae* (~5×10^6 cells/cm^3, with a depth of 0.306 cm). (*c*,*d*) Long-term development of bioconvection patterns in a suspension of *Chlamydomonas reinhardtii* (10^7 cells/cm^3, with a depth of 4 mm). (*d*) Space-time plot demonstrating the transition event. (*e*) Reversible wave number response to variation in illumination conditions from intermittent lighting (IL) to continuous lighting (CL). Panels adapted or reprinted with permission from (*a*,*b*) Williams & Bees (2011b) and (*c*–*e*) Kage et al. (2013).

where β_1 and β_2 are constants, $f(I)$ takes a similar form to $T(I)$, and $\boldsymbol{\pi}$ is a specified light direction. Thus, the torque balance becomes

$$\dot{\mathbf{p}} = \frac{1}{2B(I)}\left\{\bar{\mathbf{k}}(I,\nabla I) - [\bar{\mathbf{k}}(I,\nabla I)\cdot\mathbf{p}]\mathbf{p}\right\} + \frac{1}{2}\boldsymbol{\Omega}\times\mathbf{p} + \alpha_0\mathbf{p}\cdot\mathsf{E}\cdot(\mathsf{I}-\mathbf{pp}),$$

where $\bar{\mathbf{k}}$ in the gravitational torque term is no longer the unit vertical vector. Interestingly, the first two descriptions provided very similar linear stability results with penetrative and oscillatory

modes, despite their mechanistic differences. Different modes of instability were observed for the phototactic torque due to horizontal gradients in light intensity from self-shading driving cell flux.

Williams & Bees (2011b) performed photo-gyrotactic bioconvection experiments with *C. augustae* in variable light conditions, from above or below. They found that red light does not alter the initial pattern wavelength. However, with white light from below increasing from zero, one finds that the initial pattern wavelength at first decreases with light intensity. This is due to positive phototaxis (i.e., in this case downward) increasingly supporting a gyrotactic instability, which has the effect of drawing plumes closer together. However, beyond the critical light intensity, cells swim away from the light (negative phototaxis; upward), accumulating at the upper boundary and driving an overturning-type instability that typically has a fixed aspect ratio. Thus, the pattern wavelength does not change with further increases in light intensity.

A reorganization of long-time bioconvection patterns has been reported with red light (Kage et al. 2013) that was not observed with the initial pattern wavelength in earlier studies; these authors suggested that a photokinetic response may be responsible (**Figure 5*e***). They also reported some curious long-term pattern reorganization that has not been previously observed (**Figure 5*c*,*d***) that they ascribed to changes in cellular morphology but may also be due to variations in cell agglutinability (capacity to clump together) or life cycle. Garcia et al. (2013) investigated a phototactic but nongravitactic *Chlamydomonas* mutant. Poiseuille flow focused cells along the axis, balancing viscous torques and phototaxis. *E. gracilis* in bright illumination from below has been observed to generate concentrated patches (Suematsu et al. 2011). Phenomenological models suggest that the normally upswimming cells respond to the bright conditions by swimming normal to the light direction. Both Giometto et al. (2015) and Ogawa et al. (2016) report that the phototactic flux of *E. gracilis* depends on the gradient of a function of light intensity, say, $\phi(I)$, which with self-shading would not be inconsistent with the above results. In particular, Giometto et al. (2015) found $\phi(I) = aI(I_c - I)/(I_r + I)$ for constants a, I_r, and I_c. Annular bioconvection patterns are reported by Dervaux et al. (2017). They constructed a model for *C. reinhardtii* with phototactic torque but no gravitational torque. In their system, the light was projected in the center of a shallow suspension, which they argued leads to phototaxis directed toward the middle. Gravitational instability results in a radially symmetric bioconvective flow that supports horizontal focusing of cells swimming to the center, providing a means for positive feedback.

Another recent advance investigated the effect of light scattering on phototactic bioconvection. Ghorai et al. (2010), Panda & Ghorai (2013), Ghorai & Panda (2013), and Panda & Singh (2016) replaced the Lambert–Beer law with a radiative transfer equation for light intensity $I(\mathbf{x}, \mathbf{s}, t)$, a function of light direction $\mathbf{s}$. In essence, a fraction of the light at a point is absorbed and a fraction is scattered in a direction with probability $\Lambda(\mathbf{s}, \mathbf{s}')$, which contributes to I elsewhere. Isotropic and anisotropic scattering has been considered, which, given the large increase in complexity of the system, is best achieved numerically. The main effect is to change the base state of the system; bimodal vertical concentration profiles are possible, with knock-on consequences for modes of instability. What is less clear is how the cells should respond to the distribution of light direction at a point.

6. OXYTACTIC BIOCONVECTION

Oxytactic bacteria on average swim up gradients of oxygen of concentration C, which they consume, and accumulate at air–water interfaces, driving an overturning instability if the cells are negatively buoyant (Section 2). Hill & Pedley (2005) provided a summary of work up to the date of their review, including a formulation of models and linear stability (Hillesdon & Pedley 1996), weakly nonlinear analysis (Metcalfe & Pedley 1998) for pattern selection, and an analysis of plumes

(Metcalfe & Pedley 2001). Typically, models consist of Equations 1 and 2 with isotropic diffusion and $\mathbf{V}_c = \chi \nabla C$, where χ is a function of C or ∇C to phenomenologically control the sensitivity of cells to the chemoattractor gradient, allow chemotaxis only if there is sufficient C, and bound maximum cell speeds. An additional equation is required to describe advection, diffusion, and consumption of oxygen. More detailed descriptions seek to better represent chemotaxis with a chemotactic torque (e.g., of relevance to chemotactic bioconvection is Hopkins & Fauci 2002) and improve flux terms with generalized Taylor dispersion theory for run-and-tumble chemotaxis in a shear flow (Bearon 2003).

More recently, numerical schemes in two dimensions (Chertock et al. 2012) and three dimensions (Lee & Kim 2015) have been developed to study nonlinear dynamics, particularly the development and merging of plumes and the formation of stationary structures that recycle the cells. Chakraborty et al. (2018) considered analytical and numerical analysis of a chemotaxis system with a deformable free surface in a shallow chamber. While a curved surface is of interest for observations in suspensions of oxytactic cells in sessile drops (Tuval et al. 2005) (Section 2.1), the conditions for which a suspension could significantly deform the surface are not elucidated. Extending earlier work, Bearon & Hazel (2015) investigated the distribution of chemotactic bacteria in a simple shear flow in a channel. Notably, the continuum approach of modeling random aspects of the motion with a diffusion in physical space was unable to describe experimentally observed results of trapping in regions of high shear, casting doubt on the form of the cell conservation equation for bioconvection. There has been some progress in the formulation of energy stability methods for tackling oxytactic bioconvection problems, although there are many challenges in this technical area and opportunities for development (see Straughan 2013).

Figure 1*d* and the magnified version in **Figure 1*e*** present interesting features of oxytactic bioconvection. Black bands form perpendicular to the bioconvection rolls that appear to travel and interact. Additionally, the rolls are observed to be separated by small-scale structures. The cause of these features is an open question; systematic microscopic investigations and satisfactory explanations are absent from the literature.

7. BIOCONVECTION IN POROUS MEDIA AND MIXED CONVECTION PROBLEMS

It is surprising that despite there being no observations of bioconvection in porous media, many articles have emerged studying simple descriptions based on Darcy flow, stemming from early articles by Kuznetsov and coworkers (e.g., Kuznetsov & Jiang 2001, Kuznetsov & Avramenko 2005). However, the conclusions of Hill & Pedley (2005) remain valid: (*a*) The dynamics of swimming cells in confined spaces are complex, and boundary effects in the pores and flow-induced vorticity will undoubtedly have a major effect on gravitaxis or gyrotaxis; (*b*) observations (e.g., Pedley & Kessler 1992) indicate that bioconvection does not occur in porous media (indeed, cotton wool is used to concentrate upswimming cells to high volume fractions); and (*c*) furthermore, the critical permeability for bioconvection to occur in this system of equations is stated in the above articles to be 4×10^{-7} m^2, or 4×10^8 millidarcy. For comparison, this is at the top end of the range expected for well-sorted large gravel; the associated pore size is likely larger than current bioconvection experiments. There are, of course, very interesting aspects to do with how microorganisms negotiate pore structures and how this could be scaled up rationally to a continuum level, but studies to date have not addressed these questions.

In recent years, there have been many articles on mixed convection problems. Notable are those that combine bioconvection additively with several other instability mechanisms. Unfortunately, there are no experimental observations other than those we have discussed for salinity gradients

(Section 2). Typically, the studies involve combinations of nanoparticles, magnetohydrodynamics, vertical vibration, temperature gradients, or porous media, without due consideration of the physical and biological practicality, especially the impact on the swimming cells. These studies do not provide additional mechanistic insights into the phenomenon of bioconvection and so are not covered in this review.

SUMMARY POINTS

1. There are many observations of bioconvection across a large range of species, with growing evidence that bioconvection occurs in nature and has ecological purpose.
2. The close association between experimental and theoretical developments is a reason to celebrate this marriage of fluid dynamics and biology.
3. Models of gyrotactic bioconvection are very advanced, which has led to new understanding and generated a range of applications in other areas.
4. While models of phototaxis and chemotaxis are developing at a rapid pace, there is a gap between complex models of individual responses and modeling at a continuum level.
5. There are significant potential applications of bioconvection in industry, for which we need to embrace biological behavior to optimize processes.

FUTURE ISSUES

1. The range of validity of the flux in the cell conservation equation is not clear. Ideally, terms in the flux should be derived systematically from descriptions of populations of individuals (Hill & Bees 2002, Manela & Frankel 2003, Bearon 2003) (Section 4), but the form of the flux itself may not be justified in certain flows (Bearon et al. 2011).
2. The buoyancy term is phenomenological; it lacks a firm theoretical basis. In dilute models of bioconvection, an assumption is made that direct cell–cell interactions can be neglected. Yet at the same time, one assumes that in each small fluid element there are sufficiently many swimming cells to bestow a mean material property on the fluid, principally an increase in density. It is not clear for what range of cell concentrations and properties this assumption can be justified. Each non-neutrally buoyant cell sediments through the fluid, imparting a point force (Stokeslet) solution at leading order [see Thiffeault & Childress's (2010) discussion of mixing]. If cells are sufficiently far apart in the dilute limit that fluid flow generated by each cell does not affect that of others, how does the density difference between cells and fluid, $\Delta\rho$, lead to a meaningful average local suspension property? A multiphase model might help provide a derivation of Equation 1, but this is not without challenges.
3. Models neglect biological variation. Rotational diffusivity is already included, but even a distribution of swimming speeds has a significant effect (Bees et al. 1998). What about distributions of gravitational torque and geometry, and consideration of mixed species and internal degrees of freedom due to life history and communication?
4. Models of phototactic bioconvection are phenomenological. How do we scale up systematically from models of individuals to a continuum level? Generalized Taylor dispersion is one answer but a significant challenge.

5. Even if the cells can be considered similar, they do not swim in straight lines. Part of this has been measured and modeled, but there are other aspects that have not been properly considered in continuum bioconvection studies, such as the recently observed behavior of algae to "swim with two gears" (Polin et al. 2009) and the propensity for helical trajectories (see Section 4.5).
6. Equilibrium profiles rarely exist. Quite possibly because of the similarity between bioconvection and classical Rayleigh-Bénard convection problems, analysis of bioconvection in fluids of finite depth typically is performed about steady profiles. However, there are competing instabilities in bioconvection, not least from gyrotactic behavior, that lead to patterns and flows a long time before these profiles are approached. One answer might be non-normal stability analysis.

DISCLOSURE STATEMENT

The author is not aware of any biases that might be perceived as affecting the objectivity of this review.

ACKNOWLEDGMENTS

The author is indebted to several authors, particularly Rachel Bearon, Otti Croze, John Kessler, Stephen O'Malley, and Yoshihiro Mogami, for allowing the use of figures and photos in this review.

LITERATURE CITED

Abe T, Nakamura S, Kudo S. 2017. Bioconvection induced by bacterial chemotaxis in a capillary assay. *Biochem. Biophys. Res. Commun.* 483:277–82

Almahmud RAJ. 2016. *Wavelengths in bioconvection patterns*. PhD Thesis, Univ. Glasgow, Glasgow

Alqarni MS, Bearon RN. 2016. Transport of helical gyrotactic swimmers in channels. *Phys. Fluids* 28:071904

Anderson DM, Cembella AD, Hallegraeff GM. 2012. Progress in understanding harmful algal blooms: paradigm shifts and new technologies for research, monitoring, and management. *Annu. Rev. Mar. Sci.* 4:143–76

Ardekani MN, Sardina G, Brandt L, Karp-Boss L, Bearon RN, Variano EA. 2017. Sedimentation of elongated non-motile prolate spheroids in homogenous isotropic turbulence. *J. Fluid Mech.* 831:655–74

Bearon RN. 2003. An extension of generalized Taylor dispersion in unbounded homogeneous shear flows to run-and-tumble chemotactic bacteria. *Phys. Fluids* 15:1552–63

Bearon RN. 2013. Helical swimming can provide robust upwards transport for gravitactic single-cell algae; a mechanistic model. *J. Math. Biol.* 66:1341–59

Bearon RN, Bees MA, Croze OA. 2012. Biased swimming cells do not disperse in pipes as tracers: a population model based on microscale behaviour. *Phys. Fluids* 24:121902

Bearon RN, Grunbaum D. 2006. Bioconvection in a stratified environment: experiments and theory. *Phys. Fluids* 18:127102

Bearon RN, Hazel AL. 2015. The trapping in high-shear regions of slender bacteria undergoing chemotaxis in a channel. *J. Fluid Mech.* 771:R3

Bearon RN, Hazel AL, Thorn GJ. 2011. The spatial distribution of gyrotactic swimming micro-organisms in laminar flow fields. *J. Fluid Mech.* 680:602–35

Bees MA. 1996. *Non-linear pattern generation by swimming micro-organisms*. PhD Thesis, Univ. Leeds, Leeds

Bees MA, Croze OA. 2010. Dispersion of biased swimming micro-organisms in a fluid flowing through a tube. *Proc. R. Soc. A Math. Phys. Eng. Sci.* 466:2057–77

Bees MA, Croze OA. 2014. Mathematics for streamlined biofuel production from unicellular algae. *Biofuels* 5:53–65
Bees MA, Hill NA. 1997. Wavelengths of bioconvection patterns. *J. Exp. Biol.* 200:1515–26
Bees MA, Hill NA. 1998. Linear bioconvection in a suspension of randomly swimming, gyrotactic microorganisms. *Phys. Fluids* 10:1864–81
Bees MA, Hill NA. 1999. Non-linear bioconvection in a deep suspension of gyrotactic swimming microorganisms. *J. Math. Biol.* 38:135–68
Bees MA, Hill NA, Pedley TJ. 1998. Analytical approximations for the orientation distribution of small dipolar particles in steady shear flows. *J. Math. Biol.* 36:269–98
Bennett RR, Golestanian R. 2015. A steering mechanism for phototaxis in chlamydomonas. *J. R. Soc. Interface* 12:20141164
Cencini M, Franchino M, Santamaria E, Boffetta G. 2016. Centripetal focusing of gyrotactic phytoplankton. *J. Theor. Biol.* 399:62–70
Chakraborty S, Ivancic F, Solovchuk M, Sheu TW-S. 2018. Stability and dynamics of a chemotaxis system with deformed free-surface in a shallow chamber. *Phys. Fluids* 30:071904
Chertock A, Fellner K, Kurganov A, Lorz A, Markowich PA. 2012. Sinking, merging and stationary plumes in a coupled chemotaxis-fluid model: a high-resolution numerical approach. *J. Fluid Mech.* 694:155–90
Childress S, Levandowsky M, Spiegel EA. 1975. Pattern formation in a suspension of swimming microorganisms: equations and stability theory. *J. Fluid Mech.* 69:595–613
Clifton W, Bearon R, Bees MA. 2018. Enhanced sedimentation of elongated plankton in simple flows. *IMA J. Appl. Math.* 83:743–66
Colabrese S, Gustavsson K, Celani A, Biferale L. 2017. Flow navigation by smart microswimmers via reinforcement learning. *Phys. Rev. Lett.* 118:158004
Cortez R, Fauci L, Medovikov A. 2005. The method of regularized Stokeslets in three dimensions: analysis, validation, and application to helical swimming. *Phys. Fluids* 17:031504
Croze OA, Ashraf EE, Bees MA. 2010. Sheared bioconvection in a horizontal tube. *Phys. Biol.* 7:046001
Croze OA, Bearon RN, Bees MA. 2017. Gyrotactic swimmer dispersion in pipe flow: testing the theory. *J. Fluid Mech.* 816:481–506
Croze OA, Martinez VA, Jakuszeit T, Dell'Arciprete D, Poon WC, Bees MA. 2019. Helical and oscillatory microswimmer motility statistics from differential dynamic microscopy. *New J. Phys.* 21(6):063012
Croze OA, Sardina G, Ahmed M, Bees MA, Brandt L. 2013. Dispersion of swimming algae in laminar and turbulent channel flows: consequences for photobioreactors. *J. R. Soc. Interface* 10:20121041
Czirok A, Janosi IM, Kessler JO. 2000. Bioconvective dynamics: dependence on organism behaviour. J. Exp. Biol. 203:3345–54
Daniels R, Vanderleyden J, Michiels J. 2004. Quorum sensing and swarming migration in bacteria. *FEMS Microbiol. Rev.* 28:261–89
Delcourt J, Bode NWF, Denoel M. 2016. Collective vortex behaviors: diversity, proximate, and ultimate causes of circular animal group movements. *Q. Rev. Biol.* 91:1–24
Demetsmets R, Tomson A, Stegwee D, Van den Ende H. 1990. Cell-cell coordination in conjugating *Chlamydomonas* gametes. *Protoplasma* 155:188–99
Denissenko P, Lukaschuk S. 2007. Velocity profiles and discontinuities propagation in a pipe flow of suspension of motile microorganisms. *Phys. Lett. A* 362:298–304
Dervaux J, Resta MC, Brunet P. 2017. Light-controlled flows in active fluids. *Nat. Phys.* 13:306–13
Desai N, Ardekani AM. 2017. Modeling of active swimmer suspensions and their interactions with the environment. *Soft Matter* 13:6033–50
Diehn B, Feinleib M, Haupt W, Hildebrand E, Lenci F, Nultsch W. 1977. Terminology of behavioral responses of motile microorganisms. *Photochem. Photobiol.* 26:559–60
Drescher K, Goldstein RE, Michel N, Polin M, Tuval I. 2010. Direct measurement of the flow field around swimming microorganisms. *Phys. Rev. Lett.* 105:168101
Dunkel J, Heidenreich S, Drescher K, Wensink HH, Bär M, Goldstein RE. 2013. Fluid dynamics of bacterial turbulence. *Phys. Rev. Lett.* 110:228102

Durham WM, Climent E, Barry M, Lillo FD, Boffetta G, et al. 2013. Turbulence drives microscale patches of motile phytoplankton. *Nat. Commun.* 4:2148
Durham WM, Kessler JO, Stocker R. 2009. Disruption of vertical motility by shear triggers formation of thin phytoplankton layers. *Science* 323:1067–70
Elias S, Banin E. 2012. Multi-species biofilms: living with friendly neighbors. *FEMS Microbiol. Rev.* 36:990–1004
Flemming HC, Wingender J, Szewzyk U, Steinberg P, Rice SA, Kjelleberg S. 2016. Biofilms: an emergent form of bacterial life. *Nat. Rev. Microbiol.* 14:563–75
Garcia X, Rafaï S, Peyla P. 2013. Light control of the flow of phototactic microswimmer suspensions. *Phys. Rev. Lett.* 110:138106
Gentien P, Lunven M, Lazure P, Youenou A, Crassous MP. 2007. Motility and autotoxicity in *Karenia mikimotoi* (Dinophyceae). *Philos. Trans. R. Soc. B Biol. Sci.* 362:1937–46
Ghorai S. 2016. Gyrotactic trapping: a numerical study. *Phys. Fluids* 28:041901
Ghorai S, Hill NA. 2000. Periodic arrays of gyrotactic plumes in bioconvection. *Phys. Fluids* 12:5–22
Ghorai S, Hill NA. 2002. Axisymmetric bioconvection in a cylinder. *J. Theor. Biol.* 219:137–52
Ghorai S, Hill NA. 2005. Penetrative phototactic bioconvection. *Phys. Fluids* 17:074101
Ghorai S, Hill NA. 2007. Gyrotactic bioconvection in three dimensions. *Phys. Fluids* 19:054107
Ghorai S, Panda MK. 2013. Bioconvection in an anisotropic scattering suspension of phototactic algae. *Eur. J. Mech. B Fluids* 41:81–93
Ghorai S, Panda MK, Hill NA. 2010. Bioconvection in a suspension of isotropically scattering phototactic algae. *Phys. Fluids* 22:071901
Ghorai S, Singh R. 2009. Linear stability analysis of gyrotactic plumes. *Phys. Fluids* 21:081901
Ghorai S, Singh R, Hill NA. 2015. Wavelength selection in gyrotactic bioconvection. *Bull. Math. Biol.* 77:1166–84
Giometto A, Altermatt F, Maritan A, Stocker R, Rinaldo A. 2015. Generalized receptor law governs phototaxis in the phytoplankton *Euglena gracilis*. *PNAS* 112:7045–50
Guasto JS, Johnson KA, Gollub JP. 2010. Oscillatory flows induced by microorganisms swimming in two dimensions. *Phys. Rev. Lett.* 105:168102
Häder DP, Hemmersbach R, Lebert M. 2005. *Gravity and the Behavior of Unicellular Organisms*. Dev. Cell Biol. Ser. 40. Cambridge, UK: Cambridge Univ. Press
Hill NA, Bees MA. 2002. Taylor dispersion of gyrotactic swimming micro-organisms in a linear flow. *Phys. Fluids* 14:2598–605
Hill NA, Häder DP. 1997. A biased random walk model for the trajectories of swimming micro-organisms. *J. Theor. Biol.* 186:503–26
Hill NA, Pedley TJ. 2005. Bioconvection. *Fluid Dyn. Res.* 37:1–20
Hill NA, Pedley TJ, Kessler JO. 1989. Growth of bioconvection patterns in a suspension of gyrotactic microorganisms in a layer of finite depth. *J. Fluid Mech.* 208:509–43
Hillesdon AJ, Pedley TJ. 1996. Bioconvection in suspensions of oxytactic bacteria: linear theory. *J. Fluid Mech.* 324:223–59
Hoecker-Martinez MS, Smyth WD. 2012. Trapping of gyrotactic organisms in an unstable shear layer. *Cont. Shelf Res.* 36:8–18
Hope A, Croze OA, Poon WCK, Bees MA, Haw MD. 2016. Resonant alignment of microswimmer trajectories in oscillatory shear flows. *Phys. Rev. Fluids* 1:051201
Hopkins M, Fauci L. 2002. A computational model of the collective fluid dynamics of motile micro-organisms. *J. Fluid Mech.* 455:149–74
Hosoya C, Akiyama A, Kage A, Baba SA, Mogami Y. 2010. Reverse bioconvection of *Chlamydomonas* in the hyper-density medium. *Biol. Sci. Space* 24:145–52
Hwang Y, Pedley T. 2014a. Bioconvection under uniform shear: linear stability analysis. *J. Fluid Mech.* 738:522–62
Hwang Y, Pedley T. 2014b. Stability of downflowing gyrotactic microorganism suspensions in a two-dimensional vertical channel. *J. Fluid Mech.* 749:750–77
Ishikawa T. 2009. Suspension biomechanics of swimming microbes. J. R. Soc. Interface 6:815–34

Ishikawa T, Pedley TJ. 2014. Dispersion of model microorganisms swimming in a nonuniform suspension. *Phys. Rev. E* 90:033008

Janosi IM, Czirok A, Silhavy D, Holczinger A. 2002. Is bioconvection enhancing bacterial growth in quiescent environments? *Environ. Microbiol.* 4:525–31

Janosi IM, Kessler J, Horvath V. 1998. Onset of bioconvection in suspensions of *Bacillus subtilis*. *Phys. Rev. E* 58:4793–800

Jones MS, Le Baron L, Pedley TJ. 1994. Biflagellate gyrotaxis in a shear flow. *J. Fluid Mech.* 281:137–58

Kage A, Asato E, Chiba Y, Wada Y, Katsu-Kimura Y, et al. 2011. Gravity-dependent changes in bioconvection of *Tetrahymena* and *Chlamydomonas* during parabolic flight: increases in wave number induced by pre- and post-parabola hypergravity. *Zool. Sci.* 28:206–14

Kage A, Hosoya C, Baba SA, Mogami Y. 2013. Drastic reorganization of the bioconvection pattern of *Chlamydomonas*: quantitative analysis of the pattern transition response. *J. Exp. Biol.* 216:4557–66

Karimi A, Ardekani AM. 2013. Gyrotactic bioconvection at pycnoclines. *J. Fluid Mech.* 733:245–67

Karimi A, Paul MR. 2013. Bioconvection in spatially extended domains. *Phys. Rev. E* 87:053016

Kessler JO. 1984. Gyrotactic buoyant convection and spontaneous pattern formation in algal cell cultures. In *Nonequilibrium Cooperative Phenomena in Physics and Related Fields*, ed. MG Velarde, pp. 241–48. New York: Plenum

Kessler JO. 1985a. Co-operative and concentrative phenomena of swimming micro-organisms. *Contemp. Phys.* 26:147–66

Kessler JO. 1985b. Hydrodynamic focussing of motile algal cells. *Nature* 313:218–20

Kessler JO. 1986. Individual and collective dynamics of swimming cells. *J. Fluid Mech.* 173:191–205

Kitsunezaki S, Komori R, Harumoto T. 2007. Bioconvection and front formation of *Paramecium tetraurelia*. *Phys. Rev. E* 76:046301

Kuznetsov AV, Avramenko A. 2005. Effect of fouling on stability of bioconvection of gyrotactic microorganisms in a porous medium. *J. Porous Media* 8:45–53

Kuznetsov AV, Jiang N. 2001. Numerical investigation of bioconvection of gravitactic microorganisms in an isotropic porous medium. *Int. Commun. Heat Mass Transfer* 28:877–86

Lauga E, Powers TR. 2009. The hydrodynamics of swimming microorganisms. *Rep. Progress Phys.* 72:096601

Lee HG, Kim J. 2015. Numerical investigation of falling bacterial plumes caused by bioconvection in a three-dimensional chamber. *Eur. J. Mech. B Fluids* 52:120–30

Levandowsky M, Childress WS, Spiegel EA, Hutner SH. 1975. A mathematical model of pattern formation by swimming microorganisms. *J. Protozool.* 22:296–306

Lewis DM. 2003. The orientation of gyrotactic spheroidal micro-organisms in a homogeneous isotropic turbulent flow. *Proc. R. Soc. A Math. Phys. Eng. Sci.* 459:1293–323

Loeffer JB, Mefferd RB. 1952. Concerning pattern formation by free-swimming microorganisms. *Am. Nat.* 86:325–29

Manela A, Frankel I. 2003. Generalized Taylor dispersion in suspensions of gyrotactic swimming microorganisms. *J. Fluid Mech.* 490:99–127

Marcos, Fu HC, Powers TR, Stocker R. 2009. Separation of microscale chiral objects by shear flow. *Phys. Rev. Lett.* 102:158103

Martinez VA, Besseling R, Croze OA, Tailleur J, Reufer M, et al. 2012. Differential dynamic microscopy: a high-throughput method for characterizing the motility of microorganisms. *Biophys. J.* 103:1637–47

Mathijssen AJTM, Shendruk TN, Yeomans JM, Doostmohammadi A. 2016. Upstream swimming in microbiological flows. *Phys. Rev. Lett.* 116:028104

Mendelson N. 1999. *Bacillus subtilis* macrofibres, colonies and bioconvection patterns use different strategies to achieve multicellular organization. *Environ. Microbiol.* 1:471–77

Metcalfe AM, Pedley TJ. 1998. Bacterial bioconvection: weakly nonlinear theory for pattern selection. *J. Fluid Mech.* 370:249–70

Metcalfe AM, Pedley TJ. 2001. Falling plumes in bacterial bioconvection. *J. Fluid Mech.* 445:121–49

Mogami Y, Ishii J, Baba SA. 2001. Theoretical and experimental dissection of gravity-dependent mechanical orientation in gravitactic microorganisms. *Biol. Bull.* 201:26–33

Mogami Y, Yamane A, Gino A, Baba S. 2004. Bioconvective pattern formation of *Tetrahymena* under altered gravity. *J. Exp. Biol.* 207:3349–59
Nägeli C. 1860. Ortsbewegungen der Pflanzenzellen und ihrer Theile (Strömungen). *Beitr. Wiss. Bot.* 2:59–108
Nonaka Y, Kikuchi K, Numayama-Tsuruta K, Kage A, Ueno H, Ishikawa T. 2016. Inhomogeneous distribution of *Chlamydomonas* in a cylindrical container with a bubble plume. *Biol. Open* 5:154–60
Ochiai N, Dragiila MI, Parke JL. 2011. Pattern swimming of *Phytophthora citricola* zoospores: an example of microbial bioconvection. *Fungal Biol.* 115:228–35
Ogawa T, Shoji E, Suematsu NJ, Nishimori H, Izumi S, et al. 2016. The flux of *Euglena gracilis* cells depends on the gradient of light intensity. *PLOS ONE* 11:e0168114
O'Malley S. 2011. *Bi-flagellate swimming dynamics*. PhD thesis, Univ. Glasgow, Glasgow
O'Malley S, Bees MA. 2012. The orientation of swimming biflagellates in shear flows. *Bull. Math. Biol.* 74:232–55
Panda MK, Ghorai S. 2013. Penetrative phototactic bioconvection in an isotropic scattering suspension. *Phys. Fluids* 25:071902
Panda MK, Singh R. 2016. Penetrative phototactic bioconvection in a two-dimensional non-scattering suspension. *Phys. Fluids* 28:054105
Panda MK, Singh R, Mishra AC, Mohanty SK. 2016. Effects of both diffuse and collimated incident radiation on phototactic bioconvection. *Phys. Fluids* 28:124104
Pedley TJ. 2010. Instability of uniform micro-organism suspensions revisited. *J. Fluid Mech.* 647:335–59
Pedley TJ. 2015. Gyrotaxis in uniform vorticity. *J. Fluid Mech.* 762:R6
Pedley TJ, Hill NA, Kessler J. 1988. The growth of bioconvection patterns in a uniform suspension of gyrotactic microorganisms. *J. Fluid Mech.* 195:223–37
Pedley TJ, Kessler JO. 1987. The orientation of spheroidal micro-organisms swimming in a flow field. *Proc. R. Soc. Lond. Ser. B* 231:47–70
Pedley TJ, Kessler JO. 1990. A new continuum model for suspensions of gyrotactic micro-organisms. *J. Fluid Mech.* 212:155–82
Pedley TJ, Kessler JO. 1992. Hydrodynamic phenomena in suspensions of swimming microorganisms. *Annu. Rev. Fluid Mech.* 24:313–58
Persson A, Smith BC. 2013. Cell density-dependent swimming patterns of *Alexandrium fundyense* early stationary phase cells. *Aquat. Microb. Ecol.* 68:251–58
Platt JR. 1961. Bioconvection patterns in cultures of free-swimming organisms. *Science* 133:1766–67
Plesset M, Winet H. 1974. Bioconvection patterns in swimming microorganism cultures as an example of Rayleigh-Taylor instability. *Nature* 248:441–43
Polin M, Tuval I, Drescher K, Gollub JP, Goldstein RE. 2009. *Chlamydomonas* swims with two gears in a eukaryotic version of run-and-tumble locomotion. *Science* 325:487–90
Ramaswamy S. 2010. The mechanics and statistics of active matter. *Annu. Rev. Condens. Matter Phys.* 1:323–45
Richardson SH, Baggaley A, Hill N. 2018. Gyrotactic suppression and emergence of chaotic trajectories of swimming particles in three-dimensional flows. *Phys. Rev. Fluids* 3:023102
Roberts A. 1970. Geotaxis in motile micro-organisms. *J. Exp. Biol.* 53:687–99
Roberts A, Deacon F. 2002. Gravitaxis in motile micro-organisms: the role of fore–aft body asymmetry. *J. Fluid Mech.* 452:405–23
Sachs J. 1876. Ueber Emulsionsfiguren und Gruppirung der Schwarmsporen im Wasser. *Flora* 59:273–75
Saintillan D. 2014. Swimming in shear. *J. Fluid Mech.* 744:1–4
Santamaria F, De Lillo F, Cencini M, Boffetta G. 2014. Gyrotactic trapping in laminar and turbulent Kolmogorov flow. *Phys. Fluids* 26:111901
Sato N, Sato K, Toyoshima M. 2018. Analysis and modeling of the inverted bioconvection in *Chlamydomonas reinhardtii*: emergence of plumes from the layer of accumulated cells. *Heliyon* 4:e00586
Simha RA, Ramaswamy S. 2002. Hydrodynamic fluctuations and instabilities in ordered suspensions of self-propelled particles. *Phys. Rev. Lett.* 89:058101
Smayda TJ. 1997. Harmful algal blooms: their ecophysiology and general relevance to phytoplankton blooms in the sea. *Limnol. Oceanogr.* 42:1137–53

Sommer T, Danza F, Berg J, Sengupta A, Constantinescu G, et al. 2017. Bacteria-induced mixing in natural waters. *Geophys. Res. Lett.* 44:9424–32

Straughan B. 2013. *The Energy Method, Stability, and Nonlinear Convection*. Appl. Math. Ser. 91. New York: Springer-Verlag

Suematsu NJ, Awazu A, Izumi S, Noda S, Nakata S, Nishimori H. 2011. Localized bioconvection of *Euglena* caused by phototaxis in the lateral direction. *J. Phys. Soc. Jpn.* 80:064003

Thiffeault JL, Childress S. 2010. Stirring by swimming bodies. *Phys. Lett. A* 374:3487–90

Thorn GJ, Bearon RN. 2010. Transport of spherical gyrotactic organisms in general three-dimensional flow fields. *Phys. Fluids* 22:041902

Tuval I, Cisneros L, Dombrowski C, Wolgemuth CW, Kessler J, Goldstein RE. 2005. Bacterial swimming and oxygen transport near contact lines. *PNAS* 102:2277–82

Vincent RV, Hill NA. 1996. Bioconvection in a suspension of phototactic algae. *J. Fluid Mech.* 327:343–71

Vladimirov VA, Wu MSC, Pedley TJ, Denissenko PV, Zakhidova SG. 2004. Measurement of cell velocity distributions in populations of motile algae. *J. Exp. Biol.* 207:1203–16

Wager H. 1911. VII. On the effect of gravity upon the movements and aggregation of *Euglena viridis*, Ehrb., and other micro-organisms. *Philos. Trans. R. Soc. Lond. B* 201:333–90

Wille JJ Jr., Ehret CF. 1968. Circadian rhythm of pattern formation in populations of a free-swimming organism, *Tetrahymena*. *J. Protozool.* 15:789–92

Williams CR, Bees MA. 2011a. Photo-gyrotactic bioconvection. *J. Fluid Mech.* 678:41–86

Williams CR, Bees MA. 2011b. A tale of three taxes: photo-gyro-gravitactic bioconvection. *J. Exp. Biol.* 214:2398–408

Williams CR, Bees MA. 2014. Mechanistic modeling of sulfur-deprived photosynthesis and hydrogen production in suspensions of *Chlamydomonas reinhardtii*. *Biotechnol. Bioeng.* 111:320–35

Winet H, Jahn TL. 1972. On the origin of bioconvective fluid instabilities in *Tetrahymena* culture systems. *Biorheology* 9:87–104

Yamamoto Y, Okayama T, Sato K, Takaoki T. 1992. Relation of pattern formation to external conditions in the flagellate, *Chlamydomonas reinhardtii*. *Eur. J. Protistol.* 28:415–20

Zöttl A, Stark H. 2013. Periodic and quasiperiodic motion of an elongated microswimmer in Poiseuille flow. *Eur. Phys. J. E* 36:4

Annual Review of
Fluid Mechanics

Volume 52, 2020

Contents

Indexes

Errata

An online log of corrections to *Annual Review of Fluid Mechanics* articles may be found at http://www.annualreviews.org/errata/fluid